

# Fail-safe semi-active dynamic vibration absorber design

***Citation for published version (APA):***

Huijbers, J. H. H. (2006). *Fail-safe semi-active dynamic vibration absorber design*. (DCT rapporten; Vol. 2006.021). Technische Universiteit Eindhoven.

***Document status and date:***

Published: 01/01/2006

***Document Version:***

Publisher's PDF, also known as Version of Record (includes final page, issue and volume numbers)

***Please check the document version of this publication:***

- A submitted manuscript is the version of the article upon submission and before peer-review. There can be important differences between the submitted version and the official published version of record. People interested in the research are advised to contact the author for the final version of the publication, or visit the DOI to the publisher's website.
- The final author version and the galley proof are versions of the publication after peer review.
- The final published version features the final layout of the paper including the volume, issue and page numbers.

[Link to publication](#)

***General rights***

Copyright and moral rights for the publications made accessible in the public portal are retained by the authors and/or other copyright owners and it is a condition of accessing publications that users recognise and abide by the legal requirements associated with these rights.

- Users may download and print one copy of any publication from the public portal for the purpose of private study or research.
- You may not further distribute the material or use it for any profit-making activity or commercial gain
- You may freely distribute the URL identifying the publication in the public portal.

If the publication is distributed under the terms of Article 25fa of the Dutch Copyright Act, indicated by the "Taverne" license above, please follow below link for the End User Agreement:

[www.tue.nl/taverne](http://www.tue.nl/taverne)

***Take down policy***

If you believe that this document breaches copyright please contact us at:

[openaccess@tue.nl](mailto:openaccess@tue.nl)

providing details and we will investigate your claim.

# **Fail-Safe Semi-Active Dynamic Vibration Absorber Design**

J.H.H. Huijbers (514128)

DCT 2006.21

Traineeship report

Coach(es): F. May

Supervisor: H. Nijmeijer

Technische Universiteit Eindhoven  
Department Mechanical Engineering  
Dynamics and Control Group

Eindhoven, March, 2006



# Contents

<b>Summary</b>	<b>iii</b>
<b>1 Introduction</b>	<b>1</b>
<b>2 Theory of a dynamic vibration absorber</b>	<b>3</b>
<b>3 Types of dynamic vibration absorbers</b>	<b>5</b>
3.1 Standard passive vibration absorber . . . . .	5
3.2 Electromagnetic absorber (Proof-Mass Actuator) . . . . .	6
3.3 Piezoelectric absorber . . . . .	6
3.4 Smart spring absorber . . . . .	7
<b>4 Fail-safe semi-active dynamic vibration absorber design</b>	<b>9</b>
4.1 Are available dynamic vibration absorbers sufficient? . . . . .	9
4.2 The cup spring design . . . . .	10
4.3 Dynamic vibration absorber design based on leaf springs . . . . .	16
4.3.1 Satellite design . . . . .	16
4.3.2 Flank design . . . . .	16
<b>5 Prototype design</b>	<b>21</b>
5.1 Flank design prototype . . . . .	21
5.2 Mass moving flank design prototype . . . . .	24
<b>6 Controller design</b>	<b>29</b>

<b>7</b>	<b>Testing the design</b>	<b>35</b>
<b>8</b>	<b>Conclusions and recommendations</b>	<b>39</b>
	<b>Bibliography</b>	<b>41</b>
<b>A</b>	<b>List of symbols</b>	<b>43</b>
<b>B</b>	<b>Eigenfrequency of the satellite design</b>	<b>45</b>
<b>C</b>	<b>Transfer functions</b>	<b>51</b>
<b>D</b>	<b>Construction drawing flank design</b>	<b>55</b>
<b>E</b>	<b>Construction drawing mass moving flank design</b>	<b>57</b>
<b>F</b>	<b>Matlab code for the controller</b>	<b>59</b>
F.1	Main program: <i>controller.m</i> . . . . .	59
F.2	Processing data: function <i>detFFTqdata.m</i> . . . . .	61

# Summary

This report deals with engineering an active dynamic vibration absorber (DVA). A DVA is a construction that can be mounted on a vibrating mass to suppress the vibrations. This is achieved by setting the eigenfrequency of the DVA to the system's excitation frequency. If the excitation frequency of the system varies, an active DVA has to be used which is able to adjust its mass or its stiffness and consequently its eigenfrequency.

The aim is to create an active DVA which can easily be mounted on an existing machine. The design should be connected to a controller to adjust the eigenfrequency of the DVA automatically. It is important that the DVA is fail-safe, so it should work at least at the last controlled frequency if there is a power outage.

Three designs are proposed that all depend on varying the stiffness of the DVA. One of these designs is manufactured and a simple controller is developed.

Testing the design in practice shows that it reduces the vibration of the primary system with approximately 65 %. The DVA adapts to the excitation frequency, but the controller is slow. This is because the FRF of the masses has to be measured for about 20 s to determine the excitation frequency and the phase difference adequately. So this is the bottleneck for the controller performance. Furthermore it shows that the covered frequency range is lower than estimated, because in theory some assumptions have been made that are insufficient. For example the mass of the housing is assumed to be a point mass and inertia is neglected. Also the weight of the leaf spring is not taken into account. But the desired frequency range can easily be achieved by taking a thicker leaf spring.



# Chapter 1

## Introduction

When machines are operating they create vibrations. In some cases these vibrations have a negative influence on the performance of the machine. For instance, in a milling machine the whole construction vibrates when the grinder rotates and material is cut. This can have a negative impact on the precision of the manufactured products, the lifetime of the machine and the environment. But not only the vibrations created by the milling machine interfere with the product precision, also vibrations from outside complicate the milling process. This is why the fundament of the machine is designed very carefully. Also the bearings of the drive line and the machine tool have to be considered with care.

But there is always a difference between theory and practice. It can happen that testing the machine shows that the oscillations are higher than expected. Furthermore, the characteristics of the vibrations can differ if the vibration frequency changes or if machine characteristics vary due to for example temperature fluctuations. A solution to this problem can be found in the application of an active dynamic vibration absorber (DVA).

An active DVA is a construction that can be mounted on the vibrating machine and which is connected to a controller. Whenever the vibrational characteristics of the machine change, the controller detects this and adjusts the DVA so that the vibrations get damped as good as possible. The aim is to design a prototype of an active DVA.

It is of great importance that the functionality of the absorber is independent from current supply, so that it still works when there is no electricity ("fail-safe"). Current may only be used for the adjustment of the absorber. Therefore the design has to be mainly mechanical. The construction should be applicable widely and adjustable to frequencies in a large range. Furthermore it should be compact and simple to install so that it can be easily added to an existing mechanism. The control system for adjusting the absorber should be uncomplicated so that it is easy to handle, but it should be able to deal with nonlinearities in the exciting frequency. Finally, low power consumption and a low cost price are desirable.

For this purpose a construction has to be invented and a model has to be made. A prototype has to be manufactured before testing the design experimentally. After that, a final design



for the absorber can be established.

A testing model should be designed in which the DVA should be controlled so that its eigenfrequency follows the exciting frequency. This is easier to design than a model with changing eigenfrequencies to which the DVA is applied. Since the functionality and performance of the DVA has to be investigated, it makes no difference if the eigenfrequency of the DVA is adjusted to the exciting frequency or to the eigenfrequency of the main system. The testing model should have a base area of maximal  $(20 \times 20)\text{cm}^2$  and it should be adjustable to frequencies between 20 Hz and 30 Hz. These prescriptions are made to restrict the design process and to obtain a small prototype. In addition it should be able to add damping to the absorber and nonlinearities to the vibrations. For adjusting the DVA automatically, a controller has to be designed and optimized.

### **Problem statement:**

Design an adjustable dynamic vibration absorber with the following requirements:

- fail-safe
- large field of application (universal)
- compact
- simple to install
- able to be added to existing construction
- large frequency range in which the DVA can be applied
- uncomplicated control system
- able to deal with nonlinearities
- low cost
- low power consumption

Create a testing construction to check the performance of the DVA experimentally.

At first some examples of available DVA's are given and it is discussed whether one of these designs can be used for active dynamic vibration control due to the problem definition. It will become clear that a new design is required, so three possible constructions are proposed. Finally, one design is chosen and worked out completely. This means that it is manufactured and a controller is designed. In the end the design is tested to check if it can be applied in practice.

## Chapter 2

# Theory of a dynamic vibration absorber

The passive dynamic vibration absorber described by de Kraker and van Campen [dKvCo1] is a standard DVA invented in 1909 by Frahm [dH56]. It consists of a mass-spring system and if necessary an additional damper  $d_2$  (see figure 2.1).

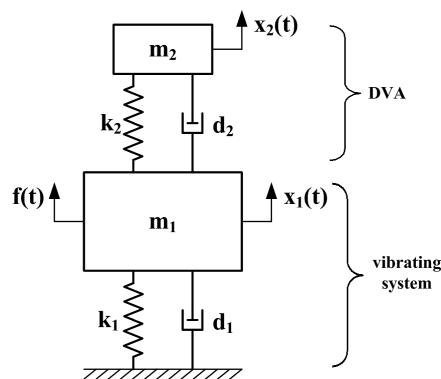


Figure 2.1: Standard passive DVA with damping

A DVA is used to reduce the vibration of a machine (primary mass  $m_1$ ) vibrating at a resonance frequency  $\sqrt{\frac{k_1}{m_1}}$  rad/s. It is mounted on the machine and its eigenfrequency is chosen to meet the resonance frequency of the primary system.

$$\frac{k_2}{k_1} = \frac{m_1 m_2}{(m_1 + m_2)^2} \quad (2.1)$$

$$\xi_2^2 = \frac{3(m_2/m_1)}{8(1 + m_2/m_1)^3} \quad (2.2)$$

The best performance (lowest resonance peaks) of the DVA is achieved for a stiffness ratio given in (2.1) and a damping ratio given in (2.2). In this way an anti-resonance is created at the eigenfrequency of the primary system, but two new resonances are created symmetrically around the antiresonance. This is shown in the next figure.

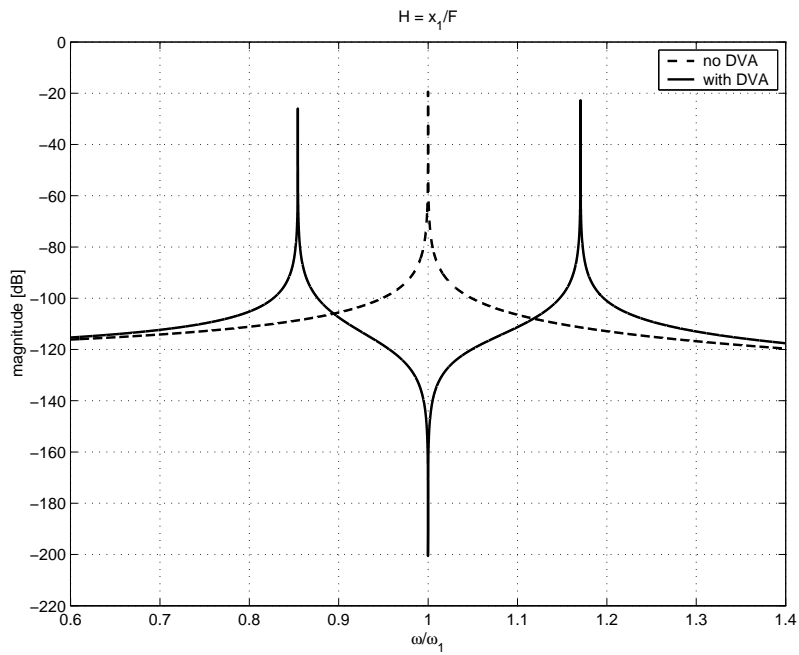


Figure 2.2: Bode plot for the transfer function of an arbitrary primary system

## Chapter 3

# Types of dynamic vibration absorbers

Before a new design is created it is investigated which types of dynamic vibration absorbers are available at the moment. This will prevent "reinventing the wheel", but it can also be a source of inspiration.

At first one has to distinguish between passive and active dynamic vibration absorbers (DVA). In contrast to active absorbers, a passive DVA has fixed system parameters and characteristics that cannot be changed during operating. Therefore it is only effective at one particular frequency. An active DVA is connected to a controller which uses sensors to survey the vibration and actuators to change the characteristics of the absorber to suppress vibrations efficiently. In this way vibrations can be neutralized in a wide range of frequencies. This kind of DVA is preferred if the excitation force is permanently varying or if the eigenfrequency of the system changes due to fluctuations in boundary conditions or temperature for instance.

There are different types of vibration absorbers available, for example standard passive dynamic vibration absorbers, electromagnetic absorbers, piezoelectric absorbers and smart spring absorbers. The choice for either one depends on the frequency range of the resonance which has to be suppressed and on the system it has to be applied to. For example a machine that is sensitive to magnetic forces cannot be damped with an electromagnetic DVA.

### 3.1 Standard passive vibration absorber

The working of the standard passive DVA is already described in the previous chapter. Once the absorber is tuned, it only neutralizes the frequency for which it is designed. If the excitation frequency changes, one has to adjust the absorber manually by increasing

or decreasing the absorber mass for instance. There is no restriction on the frequency of the resonance for which this DVA can be applied, because it can be designed the way it is needed.

### 3.2 Electromagnetic absorber (Proof-Mass Actuator)

This semi-active absorber described by Preumont [Preo2] is driven by an electromagnetic force. A sketch of a proof mass actuator can be found in figure 3.1. The permanent magnet creates a magnetic field in which the current-carrying coil with a reaction mass attached is accelerated. The reaction mass is also attached to the permanent magnet by a spring and a damper. The magnet is placed on the vibrating surface, so that the reaction mass is accelerated. By varying the current in the coil, the electromagnetic force is adjusted so that the damping of the system changes. If a controller is connected to the electromagnet, the damping of the system can be adjusted permanently. The operating field lies within a frequency range of 25 Hz to 2000 Hz [Mico5]. Note that only the damping of the system can be varied. To influence the eigenfrequency one has to change the spring constant or the reaction mass which cannot be done automatically in this design.

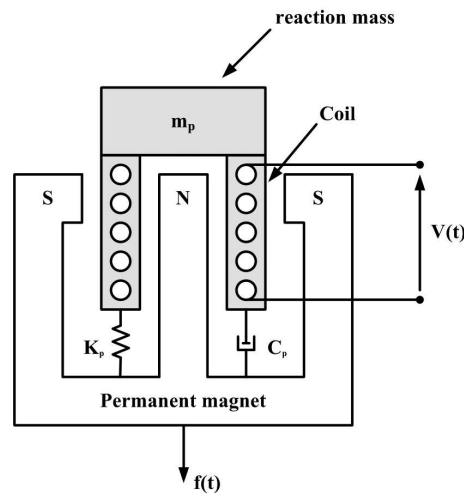


Figure 3.1: Electromagnetic DVA (Proof-Mass Actuator)

### 3.3 Piezoelectric absorber

For neutralizing unwanted vibrations, active piezoelectric absorbers can be used [Preo2]. Pairs of piezoelectric sensors and actuators are placed on the moving structure and connected to a controller. The sensors survey the local amplitudes of the vibration and the controller estimates the mode and the frequency of the vibration with this data. Then the

controller decides at which amount each actuator has to be turned on to generate a reaction force for neutralizing the vibration. Piezoelectric absorbers are small and light so they can be applied to different systems. There are different types of piezoelectric actuators that each prescribe different frequency ranges in which they work properly. Taking all ranges together, frequencies between 60 Hz and 30000 Hz can be suppressed [Pie05]. Unfortunately, the displacement capabilities of the piezoelectric actuators are limited, so that they cannot be applied to systems oscillating with large amplitudes and strong vibration forces.

### 3.4 Smart spring absorber

The smart spring (see figure 3.2) is a recently invented semi-active vibration absorber with variable structural impedance consisting of stiffness, damping and inertia [NH04] [Flao4]. The primary mass  $m_1$  (structure) is excited while the secondary mass  $m_2$ , also called the plunger, is coupled to the primary mass by piezoelectric actuators which can generate a friction force between the plunger and the primary mass. Here the piezoelectric actuators do not need large displacements and high forces at the same time to generate the required friction force which is the only cause for coupling the two mass-spring systems together. By adjusting this force the characteristics of the absorber can be changed. If the friction force is zero, the systems are uncoupled. If the friction force is sufficiently high, the systems are fully coupled. How strong the force for fully coupling the system has to be depends on the excitation force and the masses relative positions and velocities. Furthermore the friction force provides damping if the system operates between the uncoupled and fully coupled state. In this state the systems are partly coupled and there is no model that describes the connection between the eigenfrequency of the DVA and the non-linear friction force, yet. This makes controller design quite complicated. The resonance frequencies that can be damped are in the range between the eigenfrequency of the primary system and the eigenfrequency of the fully coupled system. So the design determines which resonances can be neutralized.

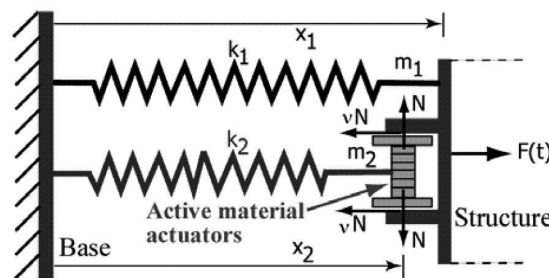


Figure 3.2: Smart spring absorber [NH04]



## Chapter 4

# Fail-safe semi-active dynamic vibration absorber design

### 4.1 Are available dynamic vibration absorbers sufficient?

The absorbers mentioned in the previous chapter will be given a closer look now. With the criterions given in chapter 1 it will become clear that a completely different design is required.

The standard passive DVA can be used for every kind of vibration. By choosing an appropriate mass, spring and damper large amplitudes can be suppressed as well as small amplitudes and the critical response frequency of the system that has to be damped can be easily shifted. In addition it is a fail safe construction, because there are no actuators that require electricity. This compact DVA can simply be added to an existing construction and is a very cheap solution for absorbing critical vibrations. But if the resonance or the exciting frequency of the vibrating system changes, this absorber is not able to adapt automatically, so that the system becomes weakly damped. This can have disastrous consequences. Therefore this kind of DVA is not appreciated if the vibrating system does not operate in steady state.

The same problem occurs with the electromagnetic absorber. It can vary the damping of the system, but it is not able to adjust the eigenfrequency automatically. The only way to change the eigenfrequency is to redesign the absorber by decreasing the reaction mass or increasing the spring constant. Thus also this kind of absorber does not match one of the main requirements, namely that the frequency of the absorber has to be automatically adjustable.

An advantage of the piezoelectric DVA is that it can easily be attached to different existing systems, because the actuators and the sensors are small and light. Furthermore this DVA is able to deal with non-linearities in the exciting frequency, because with an adequate controller it can quickly adapt its eigenfrequency. But the problem with this absorber is



its dependency on electricity. During an outage the vibrations are not neutralized since the actuators and sensors need current to suppress the vibrations. Another disadvantage lies within the limited displacement capabilities of piezoelectric devices. They cannot be applied in systems oscillating with large amplitudes and strong vibration forces.

Looking at the smart spring absorber it becomes clear that the piezoelectric devices in this design are not undergoing large displacements, since they are only used to couple two springs. The controller for this system is quite complicated, because friction has to be modeled. There is no direct transfer function between the control force input and the displacement of the main mass  $m_1$  (see figure 3.2). For example if the main mass is motionless, a non-zero control force will not result in a displacement of this mass [NH04]. Anyway, an appropriate controller can enable the system to deal with non-linearities, but the problem with outage still holds. Without electricity this DVA does not work, thus this design is not in accordance with the aim of the company.

Since all designs described above are not appreciated, something else has to be found. The principle of an adaptive DVA can be based on adjusting either the reaction mass or the stiffness. The first principle is difficult to implement while changing the stiffness of a construction is quite simple. This can be done by adding springs (like the smart spring absorber), changing springs physically (e.g. changing the length or the pre-stress of a leaf spring) or by choosing springs with exponential force-displacement curves (combination of cup springs). In the next chapter a design based on a combination of cup springs is proposed. But since the configuration of this combination extremely depends on the system the DVA has to be applied to, it is only explained in a global way. Chapter 4.3 provides two designs depending on leaf springs. In the first design the axial pre-stress of the leaf spring will be varied and in the second design the effective bending length will be changed.

## 4.2 The cup spring design

The main idea of the *cup spring design* (figure 4.1(a)) is to combine cup springs to a column of packages with increasing number of springs (see figure 4.1(c)) or a column of springs with different stiffnesses to achieve a progressive force-displacement curve. By adjusting the initial load of the springs the dynamics of the absorber can be influenced.

The inner and outer diameter of all springs are equal, but beside the pre-load their thickness and material can be varied which has an impact on the stiffness of the column, too. The columns may only be compressed, since this is the only direction in which they provide stiffness. To avoid the springs in the column from losing contact a minimal initial load  $F_v$  is required (resulting in a minimal initial column compression  $s_v$ ). The load of the springs may never go beneath  $F_v$  during operation to avoid backlash in the DVA. On the other hand the load may not exceed a certain value  $F_b$  to guarantee that the springs do not break, so the column may not be pressed further than  $s_b$ . Note that the column compression  $s$  is equal to the compression of the total cup spring column and not the displacement of the secondary mass.

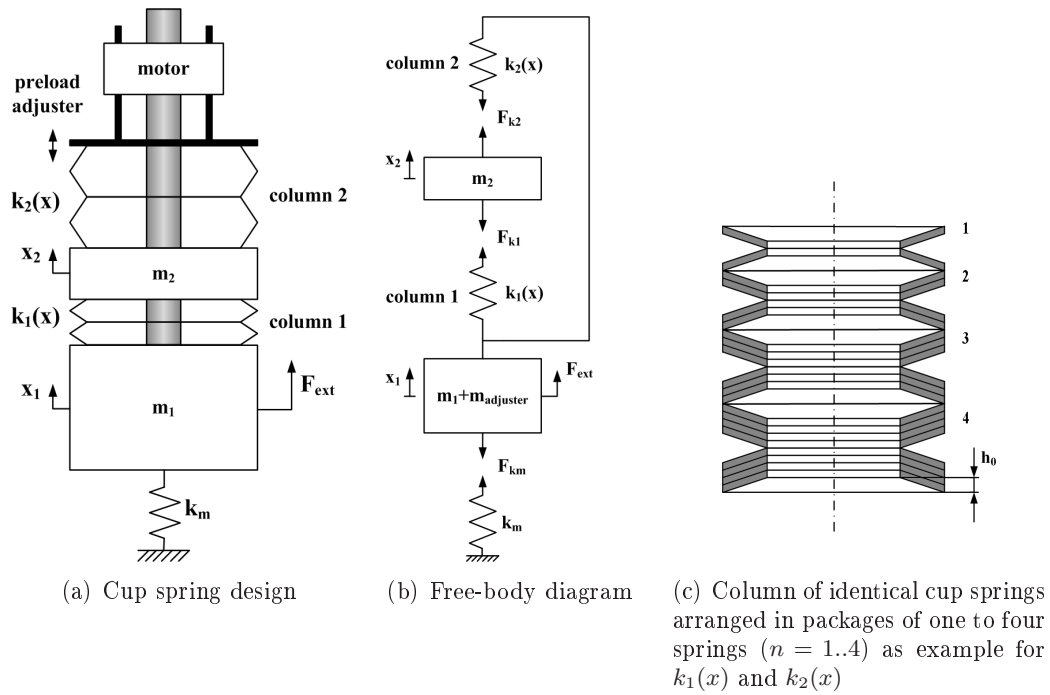


Figure 4.1: Cup spring design consisting of two columns of cup springs and a pre-load adjuster

Figure 4.2 shows the force-displacement curve of cup springs arranged in packages of one to four springs as shown in figure 4.1(c) for two different initial loads. The solid line represents the force-displacement curve of the lower column (number 1). Since there are four different spring packages in a column, there are four sections with different stiffness constants. In the first section  $[0; s_1]$  the column has the stiffness constant  $c_1$ , in the second section  $(s_1; s_2]$  stiffness  $c_2$  and so on. The displacements  $s_j$  ( $j = 1..4$ ) will be called switching points and the corresponding column forces  $F_j$  ( $j = 1..4$ ) will be called switching forces. The characteristics of the dashed line representing the upper spring column (number 2) are exactly the same as that of column 1, because both columns are identical. The line is only mirrored at the vertical through the initial displacement  $s_i$  (equilibrium point), since the columns move in opposite direction. The total stiffness of the secondary system is the sum of the stiffness of both spring columns. Since also the switching points are mirrored, the fields (I-VI) in which the total stiffness is constant are symmetric around  $s_i$ . When the system is in equilibrium ( $s_{column 1} = s_{column 2} = s_i$ ), the total stiffness of the system is  $c_2 + c_3$  for the first initial load case (solid line) and  $2c_3$  for the second initial load case (dashed line). If the mass  $m_2$  moves relatively to the primary mass for example in the downward direction, the total stiffness increases to  $c_2 + c_4$  if the exciting force is high enough so that section V is reached (in the first initial load case). Since the curves are progressive and  $c_4 > c_3$  the secondary system becomes stiffer so that its eigenfrequency increases. Because of that this design is self regulating up to a certain extend. If the initial load is adjusted, different

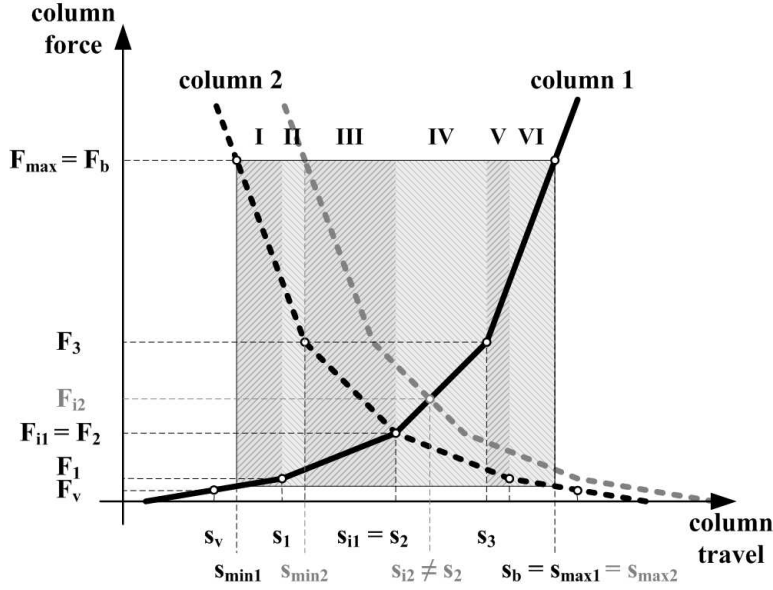


Figure 4.2: Force-displacement curve of a column of cup springs arranged in packages of one to four springs with  $s_b - s_i < s_i - s_v$  and two different initial loads

stiffness combinations can be achieved resulting in different eigenfrequencies. As already mentioned the stiffness combinations can also be influenced by varying the thickness of the cup springs.

The combination of the two requirements that the load of the springs may not fall below  $F_v$  and not exceed  $F_b$  determines the operating field of the system. If the mass  $m_2$  moves relatively to the primary mass in the downward direction, column 1 is pressed and tends to  $s_b$ , while column 2 is released and tends to  $s_v$ . In this example the first column reaches  $s_b$  earlier than the second column reaches  $s_v$ . Therefore  $s_i - s_b$  is the maximum allowed column compression symmetrically around the equilibrium position  $s_i$ . In general, the borders of the operating range are given by

$$s_{min} = s_i - \min\{(s_b - s_i), (s_i - s_v)\} \quad (4.1)$$

$$s_{max} = s_i + s_{min} \quad (4.2)$$

Here  $s_i = s_{column 1} = s_{column 2}$  is the initial spring column compression caused by the initial static load where the system is in equilibrium. For the ideal case ( $s_b - s_i = s_i - s_v$ ) this field is maximal for a specific initial load.

In principle every initial load between  $F_v$  and  $F_b$  could be applied, but it is clear that the operating range becomes smaller if the initial load is near to one of these boundaries. Another problem lies within the discrete character of the force-displacement curve. Take for

example an initial displacement between the switching points  $s_2$  and  $s_3$ . If the initial displacement is lower than the center of these switching points (figure 4.3(a)), a dip occurs in the total stiffness if section II or V is reached (figure 4.4(a)). The same happens in section I and VI (figure 4.3(a) and 4.4(c)) if the initial displacement is larger than the center of the switching points. A dip in the total stiffness results in a decrease of the suppressing force. So if the exciting force is large enough to reach the next section, the reaction force suddenly decreases. This can cause the system to break, since the mass is not slowed down enough anymore. If the initial displacement is in the center of the switching points, sections II and V vanish and there is no dip in the stiffness anymore (see figure 4.4(b)). The same holds for an initial displacement equal to a switching point. Thus not every initial load is appreciated, but only initial loads equal to switching loads or loads corresponding to initial displacements in the center of two switching points. In this way a dip in the stiffness of the secondary system is prevented. For  $n$  different spring packages in a column this results in  $2n - 1$  appropriate initial loads. Note that in this example the combination of the springs is chosen to meet  $c_2 + c_4 > 2c_3$ .

The displacements  $x_j$  ( $j = 1; 2$ ) of the vibrating masses are measured relatively to the unexcited but pre-stressed case where the upward direction is taken positive. Therefore  $x_j = 0$  corresponds to a column compression  $s_{col_j} = s_i$  which is the equilibrium point of the system, so the actual column compression  $s_{col_j}$  is given by  $s_{col_1} = s_i + x_1 - x_2$  for column 1 and  $s_{col_2} = s_i - x_1 + x_2$  for column 2. Remember that the column compression  $s$  describes the amount at which a column is pressed. Since the initial load is applied only at column 2, the absolute equilibrium position of the secondary mass changes if the initial load is varied, but  $x_1 = x_2 = 0$  still stays the equilibrium point of the system at which  $s_{col_1} = s_{col_2} = s_i$ .

The equations of motion for this design are derived with the free-body diagram 4.1(b). They are given by

$$\begin{cases} (m_1 + m_{adj})\ddot{x}_1 + [k_m + k_1(s_{col_1})]x_1 - k_1(s_{col_1})x_2 = F_{ext} \\ m_2\ddot{x}_2 - k_1(s_{col_1})x_1 + [k_1(s_{col_1}) + k_2(s_{col_2})]x_2 = 0 \end{cases} \quad (4.3)$$

According to figure 4.2 the variable spring stiffnesses  $k_1(s_{col_1})$  and  $k_2(s_{col_2})$  are functions of the actual column compressions  $s_{col_1}$  and  $s_{col_2}$  which depend on the position  $x_1$  and  $x_2$  of the masses  $m_1$  and  $m_2$  respectively and the initial displacement  $s_i$  as described earlier. Consequently the stiffness of the columns depends on the initial load. Therefore the eigenfrequency of the system can be influenced by the initial displacement.

The stiffness of a spring column with four different spring packages is given by

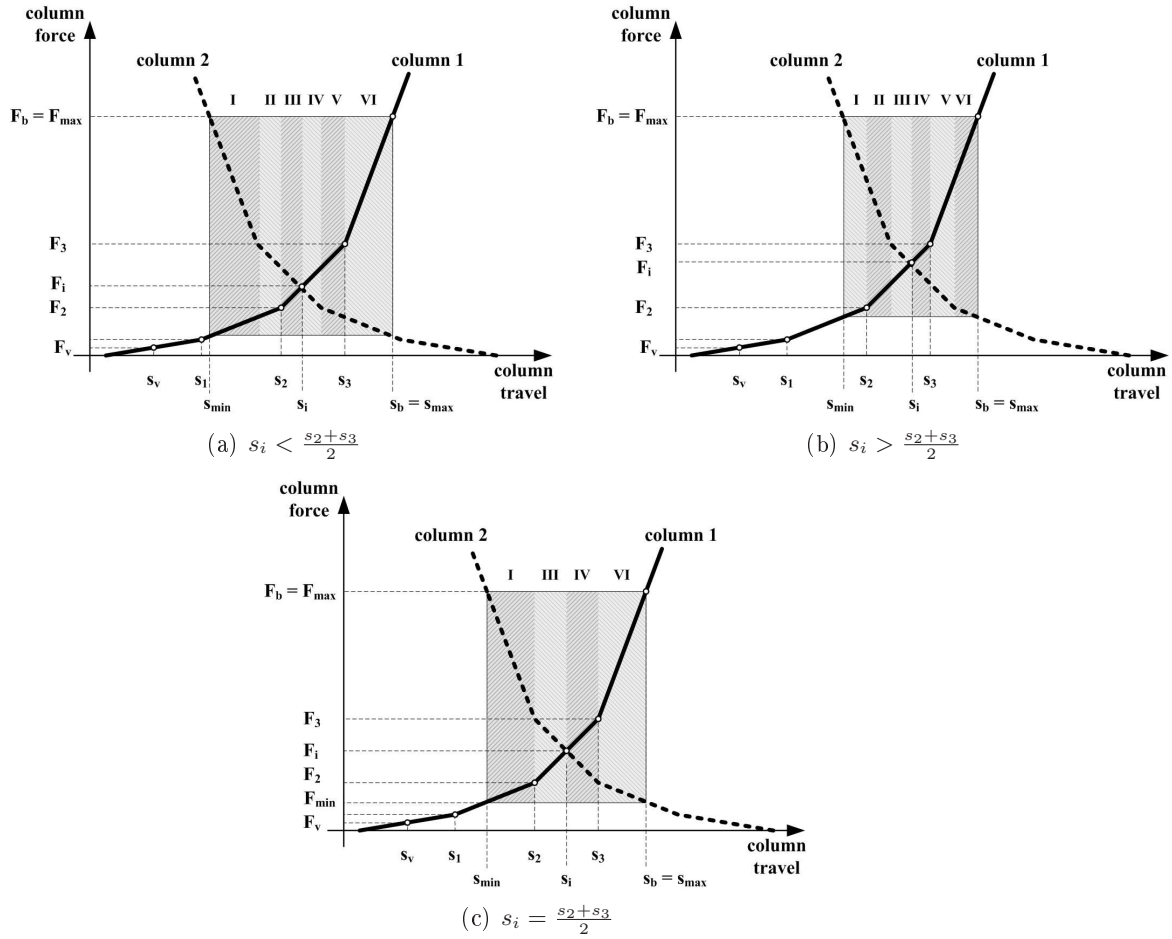


Figure 4.3: Force-displacement curves for different initial displacements

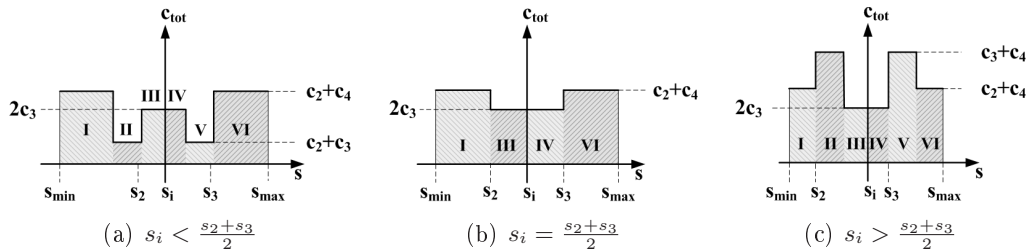


Figure 4.4: Influence of the initial displacement  $s_i$  on the stiffness of the secondary system

$$c(s) = \begin{cases} c_1 & \text{for } s_v < s \leq s_1 \\ c_2 & \text{for } s_1 < s \leq s_2 \\ c_3 & \text{for } s_2 < s \leq s_3 \\ c_4 & \text{for } s_3 < s \leq s_b \end{cases} \quad (4.4)$$

with  $0 < s_v < s_1 < s_2 < s_3 < s_b$   
and  $0 < c_1 < c_2 < c_3 < c_4$

As an example the equations of motion are given for the force-displacement curve of figure 4.2 where  $s_i = s_2$ .

$$I : \begin{cases} (m_1 + m_{adj})\ddot{x}_1 + [k_m + c_1]x_1 - c_1x_2 = F_{ext} \\ m_2\ddot{x}_2 - c_1x_1 + [c_1 + c_4]x_2 = 0 \end{cases} \quad (4.5)$$

for  $s_{min} - s_i < x_1 - x_2 \leq s_1 - s_i$

$$II : \begin{cases} (m_1 + m_{adj})\ddot{x}_1 + [k_m + c_2]x_1 - c_2x_2 = F_{ext} \\ m_2\ddot{x}_2 - c_2x_1 + [c_2 + c_4]x_2 = 0 \end{cases} \quad (4.6)$$

for  $s_1 - s_i < x_1 - x_2 \leq s_i - s_3$

$$III : \begin{cases} (m_1 + m_{adj})\ddot{x}_1 + [k_m + c_2]x_1 - c_2x_2 = F_{ext} \\ m_2\ddot{x}_2 - c_2x_1 + [c_2 + c_3]x_2 = 0 \end{cases} \quad (4.7)$$

for  $s_i - s_3 < x_1 - x_2 \leq 0$

$$IV : \begin{cases} (m_1 + m_{adj})\ddot{x}_1 + [k_m + c_3]x_1 - c_3x_2 = F_{ext} \\ m_2\ddot{x}_2 - c_3x_1 + [c_3 + c_2]x_2 = 0 \end{cases} \quad (4.8)$$

for  $0 < x_1 - x_2 \leq s_3 - s_i$

$$V : \begin{cases} (m_1 + m_{adj})\ddot{x}_1 + [k_m + c_4]x_1 - c_4x_2 = F_{ext} \\ m_2\ddot{x}_2 - c_4x_1 + [c_4 + c_2]x_2 = 0 \end{cases} \quad (4.9)$$

for  $s_3 - s_i < x_1 - x_2 \leq s_i - s_1$

$$VI : \begin{cases} (m_1 + m_{adj})\ddot{x}_1 + [k_m + c_4]x_1 - c_4x_2 = F_{ext} \\ m_2\ddot{x}_2 - c_4x_1 + [c_4 + c_1]x_2 = 0 \end{cases} \quad (4.10)$$

for  $s_i - s_1 < x_1 - x_2 < s_{max} - s_i$

So for this example there are six sets of linear differential equations which are only valid for specific relative displacements  $x_1 - x_2$ . Depending on the characteristics of the force-displacement curve and the initial load one obtains a couple of sets of two linear equations of motion that each are only valid on a specific trajectory  $\mathcal{F} = \{x_1, x_2 \in f(s_{col1}, s_{col2})\}$ . If there are more different cup springs in a column, the number of sets will increase. Furthermore the trajectories change if the initial load is varied. So the dynamics of the system can easily be described for particular cases, but globally it becomes quite complex. If the cup spring DVA has to be designed, the primary system and the characteristics of

the vibration have to be investigated very carefully to determine an adequate combination of cup springs. After that, the dynamics of the designed DVA can be described. So this design is not universal. At the moment the company has not yet defined a system to which the DVA has to be applied to. Therefore the cup spring design is put aside.

### 4.3 Dynamic vibration absorber design based on leaf springs

In this chapter two different designs for adjustable DVAs will be suggested which both are based on the fact that the bending stiffness of leaf springs can easily be changed. Just to name the constructions the first design will be called *satellite design* and the second *flank design*.

#### 4.3.1 Satellite design

The satellite design shown in figure 4.5 consists of a leaf springs with a mass mounted at the center. The ends of the spring are linked to two arms. The arms can be stretched by a two equal spindles, so that the leaf springs are charged under tensile stress. This will increase the stiffness of the springs and consequently the eigenfrequency of the construction. The spindles are connected to a self inhibiting worm gear, driven by a motor. Since the leaf spring is made of metal, high forces are required to adjust the eigenfrequency of the system. A problem can be to set these forces precisely, because the spring is lengthened only a fraction of a millimeter. Therefore the drive will need a large reduction.

The derivation for the eigenfrequency of the satellite design can be found in appendix B. Unfortunately no symbolic equation for the eigenfrequency subject to the pre-load and the design geometry can be derived. Only if all parameters are given, the eigenfrequency can be estimated numerically. The strategy to come to a construction would be to first determine an adequate geometry for the unstressed case to damp a frequency of for example 15 Hz if the spring is not pre-loaded. This will be the lowest frequency that can be damped, since the tensile pre-load will only increase the eigenfrequency of the DVA. After that the required force to cover the desired frequency range can be estimated. Then it can be decided, whether it was a good choice for the geometry. If not, the computation can be done again for a different geometry.

#### 4.3.2 Flank design

The flank design shown in figure 4.6(a) consists of a supporting construction, one large and two small leaf springs and two equal masses. The leaf springs are mounted on guidances on the supporting construction and clamped by rolls. The rolls are driven by a motor so that the effective bending length of the leaf springs can be adjusted. At the end of the springs a mass is located. By moving the leaf springs, the length over which they bend

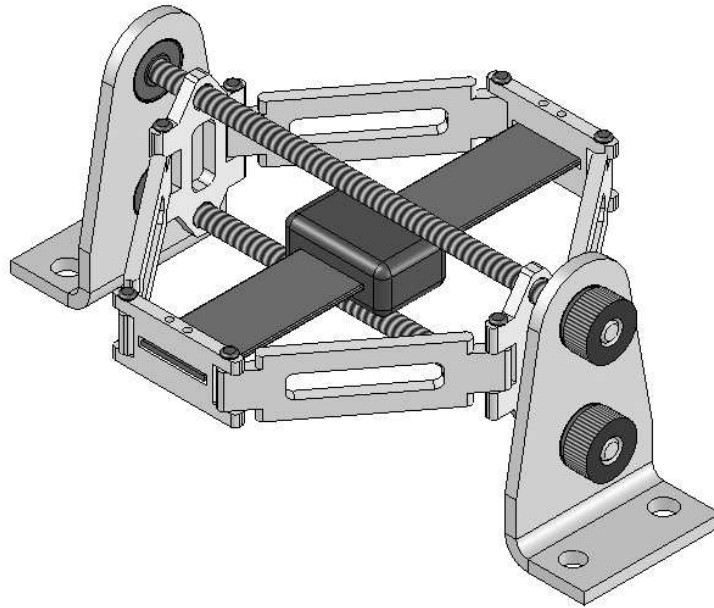


Figure 4.5: Satellite design

changes and consequently their stiffness and their natural frequency, too. For symmetry reasons not only the reaction masses are the same on both sides, but also the thickness and the effective lengths of the springs. The width of each small spring  $b_s$  is half the width of the large spring  $b_l$ , so the total mass-spring system is the same on both sides. Therefore a characteristic width  $b$  is introduced and defined as  $b = b_l = 2b_s$ . The reason for splitting one spring is symmetry to avoid moments around the horizontal axis.

Simulations have already confirmed that the dynamic behavior of this kind of DVA is almost equal to that of a single DOF mass-spring system [BFNo4]. Therefore it is modeled as a simple mass-spring system with variable stiffness (see figure 4.6(b)).

Since both reaction masses and effective lengths of the springs are desired to be equal one could think of taking the secondary mass-spring systems together and model just a single secondary system. But it can happen that the effective length of the leaf springs is not exactly the same on either side due to differences in the driving mechanism. On the other hand one can possibly neutralize different harmonics by purposely keeping the effective lengths different. Note that this will introduce a moment around the x-axis. These effects can be investigated with separately modeled reaction masses and leaf springs and the performance of the DVA can be determined. This leads to the following equations of motion



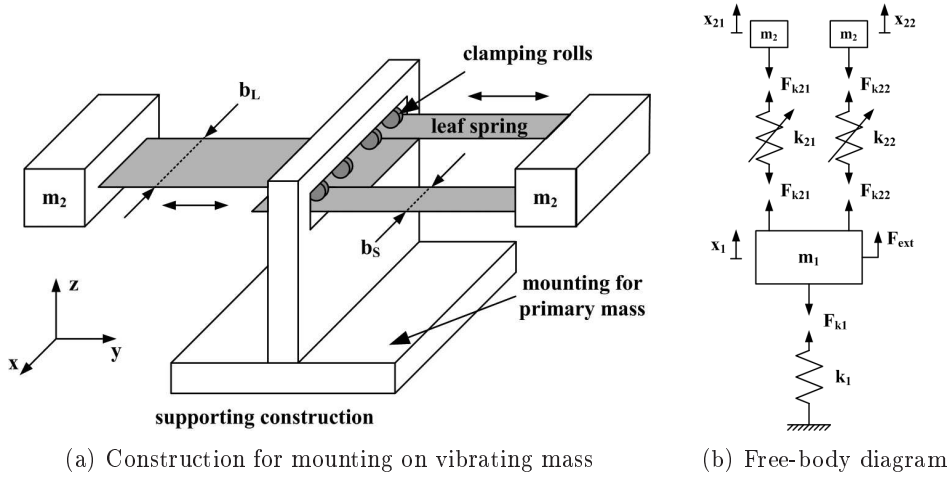


Figure 4.6: Flank design

$$\begin{cases} m_1 \ddot{x}_1 + (k_1 + k_{21} + k_{22})x_1 - k_{21}x_{21} - k_{22}x_{22} = F_{ext} \\ m_{21} \ddot{x}_{21} + k_{21}(x_{21} - x_1) = 0 \\ m_{22} \ddot{x}_{22} + k_{22}(x_{22} - x_1) = 0 \end{cases} \quad (4.11)$$

Note that the mass  $m_1$  is the sum of the mass of the vibrating system and the supporting construction. The eigenfrequencies of the mass-spring systems are

$$\omega_{e1} = \sqrt{\frac{k_1}{m_1}} \quad \omega_{e21} = \sqrt{\frac{k_{21}}{m_{21}}} \quad \omega_{e22} = \sqrt{\frac{k_{22}}{m_{22}}}$$

The DVA works properly if mass and stiffness of the secondary systems are tuned so that  $\omega_{e1} = \omega_{e21} = \omega_{e22}$ . If the eigenfrequency of the primary system changes, the stiffness of the secondary systems can be adjusted by changing the effective length of the leaf springs to achieve the same eigenfrequency. Another option is to adjust the eigenfrequency of the DVA to the excitation frequency. According to Holzweissig and Dresig [HD79] the stiffness constant of a rectangular cantilever spring with one free end (see figure 4.7) is given by

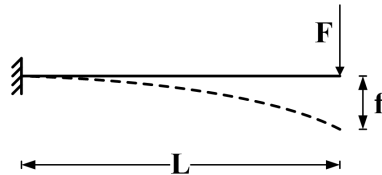


Figure 4.7: Free cantilever spring for flank design

$$c = \frac{F}{f} = 3 \frac{EI}{l^3} = \frac{Ebh^3}{4l^3} \quad (4.12)$$

So the eigenfrequencies of the secondary systems  $\omega_{e21}$  and  $\omega_{e22}$  become

$$\omega_{e21} = \sqrt{\frac{Ebh^3}{4m_{21}l_{21}^3}} \quad \omega_{e22} = \sqrt{\frac{Ebh^3}{4m_{22}l_{22}^3}} \quad (4.13)$$

Now it is obvious that by changing the effective length of the leaf spring the eigenfrequency of the system can be adjusted. The longer the spring, the lower the eigenfrequency. Note that the mass of the leaf springs is neglected here, because it is assumed to be much lighter than the secondary mass  $m_2$ . Equation (4.13) can be rearranged to determine the effective lengths required to adjust the eigenfrequencies of the secondary systems to the eigenfrequency of the primary system:

$$l_{21} = \left( \frac{Ebh^3}{4m_{21}\omega_{e1}^2} \right)^{\frac{1}{3}} \quad l_{22} = \left( \frac{Ebh^3}{4m_{22}\omega_{e1}^2} \right)^{\frac{1}{3}} \quad (4.14)$$

When the eigenfrequency of the primary system  $\omega_{e1}$  is substituted by the excitation frequency, the eigenfrequency of the DVA can be set to the exciting frequency. It is important to mention that the dimensions of the leaf springs and the secondary masses should be tuned very carefully to obtain a compact design and the best neutralizing effect. Normally, the total secondary mass is chosen to be between 5 % and 10 % of the primary mass, which means that  $0,025m_1 \leq m_{2i} \leq 0,05m_1$ ,  $i = 1; 2$ . Furthermore the stress in either spring has to be calculated to avoid breaking. It is maximal at the clamping point and given by [HD79]

$$\sigma_{b,max} = 3 \frac{EI}{W} \frac{f}{l^2} = \frac{3Ehf}{2l^2} \quad \text{for } \frac{f}{l} \leq 0.3 \quad (4.15)$$

This bending stress may not exceed the maximal allowed dynamic bending stress  $\sigma_{b,W} \approx 6 \cdot 10^8$  Pa for spring steel to prevent plastic deformation, fatigue and breaking. This holds for steel Ck 75 (DIN 17222). The deflection  $f$  of either spring is equal to the maximal displacement  $x_{21}$  and  $x_{22}$  respectively (figure 4.6(b)). Depending on the difference in the effective lengths of the springs, the maximal displacement  $x_{21}$  or  $x_{22}$  decides at which side of the DVA the maximal allowed dynamic bending stress is reached first. Note that (4.15) only holds for a deflection rate  $\frac{f}{l} \leq 0.3$ . For larger deflections the stress-displacement curve increases faster and has a non-linear character so that the stress can only be determined with a lookup table.

Unfortunately there was not enough time left to work out two designs. Therefore a construction is built only for the flank design and the satellite design is put aside.



## Chapter 5

# Prototype design

This chapter explains how to implement the flank and the satellite design for practical application. A prototype for either design is developed for testing their performance in practice. As mentioned in the problem definition (see chapter 1) the base area should not exceed  $(20 \times 20) \text{ cm}^2$ . The aim is to keep the bearing construction of the DVA that is mounted on the primary mass as light as possible, to affect the eigenfrequency of the primary system as less as possible. Therefore many parts will be made of hard plastic. The total DVA (bearing construction plus secondary system) should be about 10 % of the weight of the primary system.

### 5.1 Flank design prototype

A construction drawing for the flank design can be found in appendix D. The torque of the motor is transmitted by belts. Also on the leaf springs a belt is glued. This belt is driven by a pulley to adjust the effective bending length of the springs. Note that the belt will provide damping to the DVA because of friction between belt, glue and leaf spring when the DVA is operating. The weight of this design is between 1,5 kg and 2 kg, due to the motor that is used. The required torque of the drive depends on the secondary masses  $m_{21}$  and  $m_{22}$ , the length of the leaf springs and the gear reduction. Assuming for efficiency reasons that the weight of the secondary system is at least the weight of the bearing construction implies that  $m_{21} = m_{22} = 1 \text{ kg}$ . Thus the primary mass of the prototype has to be 40 kg plus 2 kg for the supporting construction of the DVA for the case that the DVA is mounted, so that the weight of the total DVA is 10 % of the weight of the original system. Without DVA the primary mass will just be 40 kg.

The exciting frequency varies between 20 Hz and 30 Hz. To keep the testing model simple the eigenfrequency of the primary mass should be chosen higher than 30 Hz so that there are no resonances of the primary mass that could disturb the DVA in adjusting to the exciting frequency. But of course the DVA should work at the resonance frequency of the

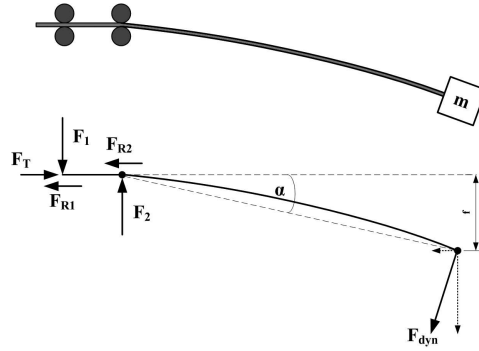


Figure 5.1: Load case for the flank design

primary mass, too. For an eigenfrequency of 35 Hz the primary spring stiffness  $k_1$  should be about  $2 \cdot 10^6$  N/m. With (4.14) the required length of the leaf springs to cover the frequency range is estimated. The total width of the springs is 90 mm and they are made of spring steel with an E-modulus of  $2,1 \cdot 10^{11}$  Pa and a maximal dynamic bending stress of  $6 \cdot 10^8$  Pa. A thickness of 1,2 mm results in a required spring length of 48 mm for 30 Hz and 64 mm for 20 Hz. The maximum length of the springs is 80 mm, so the design can achieve lower frequencies than 20 Hz as well as frequencies higher than 30 Hz without exceeding the maximal allowed stress. But for high frequencies the length of the springs has to be set precisely, because for example the difference between 60 Hz and 70 Hz is only 2 mm.

To determine the required torque of the motor to be able to adjust the effective length of the leaf springs the friction forces of the guiding rolls have to be estimated. The load case is drawn in figure 5.1. The clamping force should be large enough to prevent the leaf springs from losing contact to the rolls, but it should not be too high to keep the required motor torque for changing the effective bending length as low as possible. For the same reason the friction between the rolls and the leaf springs should be very low, although slip should be avoided.

The friction constant between steel and steel is 0,1 [RM87] for the lubricated case. So the friction forces  $F_{R1}$  and  $F_{R2}$  are given by  $0,1F_1$  and  $0,1F_2$  respectively. Therefore the total friction force that has to be overcome by the gearing is the sum of these friction forces and a small pre-load force for each pair of guiding rolls. This sum is the required gear force  $F_T$  at the leaf driving gearwheel, if the leaf springs are in horizontal position. But the length of the springs should be adjustable if the masses are vibrating, too. For small displacements one can assume that  $\tan \alpha = f/l$ , where  $f$  is the vertical displacement of the secondary mass which is not more than 1,5 mm at 30 Hz, according to simulations with an excitation force of 20 N. This leads to a maximal acceleration  $a_{dyn} = 1,5mm \cdot \omega^2 = 50m/s^2$  and a maximal dynamic bending stress of  $2 \cdot 10^8$  Pa. Due to the requirement for the base area that limits the dimensions of the design the length  $l$  of the spring is maximal 7,5 cm and the distance  $a$  between the guiding rolls is about 2 cm. This results in a maximal angle  $\alpha = 1^\circ$ , so  $\sin \alpha \approx 0$  and  $\cos \alpha \approx 1$ . Therefore the horizontal component of the dynamic force can be left out.

Neglecting the pre-load force this leads to (5.1) and (5.2) with  $F_{dyn} = m \cdot a_{dyn} = 50N$ .

$$F_1 = \frac{l}{a} F_{dyn} \quad (5.1)$$

$$F_2 = \frac{a+l}{a} F_{dyn} \quad (5.2)$$

For a driving wheel diameter of 48 mm this results in a maximal required torque of approximately 1 Nm for both leaf driving gearwheels in the design (see (5.3)). The required motor torque depends on the transmission of the gearing that still has to be chosen. To avoid the springs from slipping out of the supporting construction the gearing has to be self-inhibiting or a mechanical brake has to be mounted on the motor.

$$\begin{aligned} T &= F_T \cdot r \\ &= (F_{R_1} + F_{R_2}) \cdot r \\ &= (0,1F_1 + 0,1F_2) \cdot r \\ &= 0,1 \frac{2l+a}{a} m \cdot a_{dyn} \cdot r \end{aligned} \quad (5.3)$$

With a gear reduction of 2,73:1 provided by the pulleys and 100:1 provided by the plastic gearing mounted on the motor, the total reduction of the drive line is 273:1. The inertia of the drive line is neglected, because the pulleys are made of plastic so they are very light. Taking losses in the drive line and the pre-load of the guiding rolls into account, a motor with a continuous torque of 23,5 mNm is chosen since this is the smallest standard motor to which a brake can be added. So the constant drive torque is maximal 6,4 Nm which is more than a factor 6 higher than required and it will be no problem to overcome the pre-load of the guiding rolls and the losses in the drive line. Together with the plastic planet gearing and a brake the mass of the motor is about 300 g. The total weight of the construction will be about 1,9 kg.

But this construction has two problems. At first the drive belts (pitch 2,5 mm, width 6 mm) cannot transmit the required torque, because the stress on the teeth is too high since the belts are too small. There is only space for belts with 5 mm pitch and 10 mm width which theoretically could transmit the torque, but there is no safety factor. A solution could be to use strong cog wheels instead of pulleys and belts, but this kind of wheels are expensive. Another disadvantage of this design is that clamping and bending point of the leaf spring are the same. Since the bending stress is maximal at the bending point and an additional stress due to the clamping is acting at the same point, this can cause breaking of the springs. It would be better to separate the clamping point and the point where the bending stress is maximal by choosing a different spring geometry, but this is impossible with this kind of design.

Driven by these problems an other construction based on the same DVA principle is proposed. The leaf springs will be clamped at a fixed length and the secondary masses will be forced to move along the leaf springs. The new design will be called *mass moving flank design* (MMF design). This construction provides some advantages compared to the flank design which will become clear in the next section.

## 5.2 Mass moving flank design prototype

The theory of the MMF design (figure 5.2) is the same as described for the flank design in chapter 4.3.2. The difference lies within the construction of the designs. In the flank design the effective bending length of the leaf springs is changed by adjusting the clamping point of the leaf springs, whereas in the MMF design this is done by moving the secondary masses along the leaf springs. An advantage of the MMF design is that clamping point and bending point can be separated by choosing an adequate spring geometry (see figure 5.3(a)), so that the stress in the springs is allocated better. This will decrease the chance of breaking and guarantees a longer life of the spring. In addition the length of the springs can be chosen longer, because they are arranged differently. As a result the eigenfrequencies of the DVA that can be set lie within a larger range. Furthermore the drive is not mounted on the bearing construction, but on the secondary mass. So its weight contributes to the secondary mass. This leads to a lighter bearing construction and finally a lighter DVA. The construction drawing of this design can be found in appendix E.

The strategy to determine all relevant design parameters is the same as followed for prototyping the flank design. At first the constraints for all parameters have to be listed. The base area is  $(200 \times 200) \text{ mm}^2$  and the DVA should operate between 20 Hz and 30 Hz. The weight of the primary system is chosen to be 20 kg, so the weight of the construction that is mounted on the primary mass should not exceed 2 kg, which is 10 % of the primary

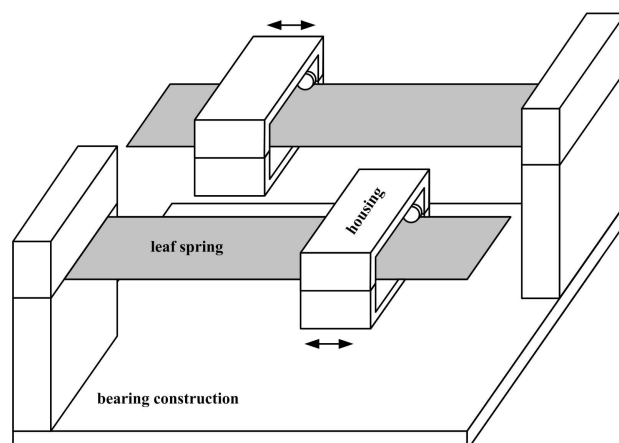


Figure 5.2: Outline of the MMF desing

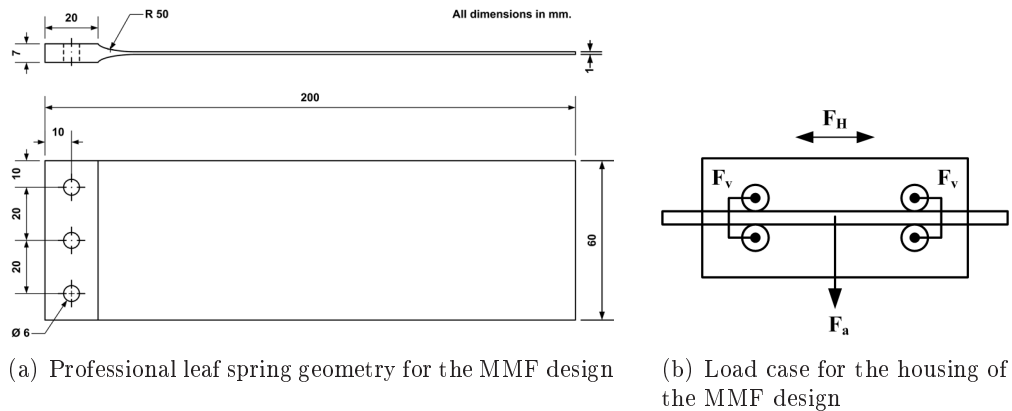


Figure 5.3: Components of the MMF design

mass. In this way the eigenfrequency of the primary system is not affected too much. For the bearing construction of the DVA 1 kg is reserved, so the secondary masses  $m_{21}$  and  $m_{22}$  should not exceed 0,5 kg each. The lowest eigenfrequency of the primary system is chosen to be about 35 Hz which is higher than the maximal frequency the DVA has to adjust to. This results in a primary spring stiffness of approximately  $10^6$  N/m. In this way resonances of the primary mass in the design region are avoided. Remember that the DVA is designed to follow the exciting frequency and not to neutralize the eigenfrequency of the primary system, so that the mass and the stiffness of the primary system can be kept constant.

According to the base area of  $200 \times 200 \text{ mm}^2$  the effective length of the leaf springs is maximal 120 mm, since the thickness of the clamping device for the leaf spring is chosen to be 20 mm and at least 60 mm are required for the housing of the drive (see the construction drawing in appendix E). The width of the springs is chosen to be 60 mm to have little space left between the housings. Choosing a leaf spring thickness of 1 mm the range for the effective length of the leaf springs required to set the eigenfrequencies of the DVA between 20 Hz and 30 Hz can be determined with (4.14). The mass of one leaf spring is 94 g. This is 19 % of the mass of one housing so that the assumption that the leaf springs are massless possibly is wrong. Unfortunately the spring thickness is so small, that it would be very expensive to create the spring geometry as shown in figure 5.3(a). Therefore a simple leaf spring is chosen. For covering the desired frequency range the effective spring length lies between 55 mm and 75 mm. Since the length of the springs is not totally used, there is still space left to set lower frequencies as well as higher. The modal damping in the construction is assumed to be 0,02 resulting from damping in the drive line and the joints. The static displacement of the housing is less than 2 mm.

The excitation force  $F_{ext}$  is chosen to be 20 N (10 % of the gravitational force of  $m_1$ ). It will be provided by a motor with an unbalance mounted on the primary mass. For the design process it is assumed that both wings of the DVA are set to the same frequency. Therefore  $x_{21} = x_{22} = x_2$ . The transfer functions  $H_1 = x_1/F_{ext}$  and  $H_2 = x_2/F_{ext}$  for the case that the DVA is mounted can be derived from the equations of motion ((4.11)) as shown in



appendix C. From the bode plots (figure 5.4 and 5.5) the amplitudes  $x_1$ ,  $x_{21}$  and  $x_{22}$  for the DVA adjusted to 20 Hz and 30 Hz can be determined. At 20 Hz the amplitude of the primary mass is  $0,45 \mu\text{m}$  ( $x_1/F_{ext} = -153 \text{ dB}$ ) and the deflection of the secondary mass is  $1,6 \text{ mm}$  ( $x_2/F_{ext} = -82 \text{ dB}$ ). At 30 Hz  $x_1 = 0,06 \mu\text{m}$  ( $x_1/F_{ext} = -170 \text{ dB}$ ) and  $x_2 = 0,6 \text{ mm}$  ( $x_2/F_{ext} = -90 \text{ dB}$ ). But if the exciting frequency suddenly changes to the resonance of the DVA in the mounted case and if the DVA does not adapt fast enough, the amplitudes will be higher. For safety reasons the maximal amplitude of the secondary masses  $\hat{x}_2$  is set to  $4 \text{ mm}$  at 30 Hz ( $-74 \text{ dB}$ ). This results in a maximal acceleration of  $\hat{a} = \hat{x}_2 \cdot \omega^2 = 142 \text{ m/s}^2$ . According to (4.15) the corresponding maximal bending stress of the leaf spring is  $4,2 \cdot 10^8 \text{ Pa}$  (at the clamping point) which is below the maximal allowed value of  $6 \cdot 10^8 \text{ Pa}$ .

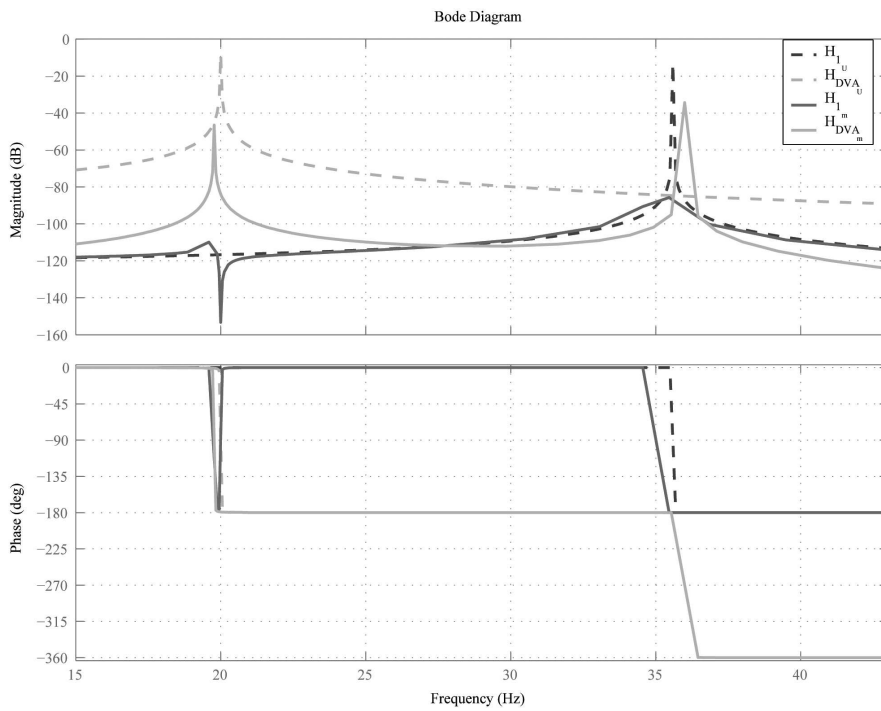
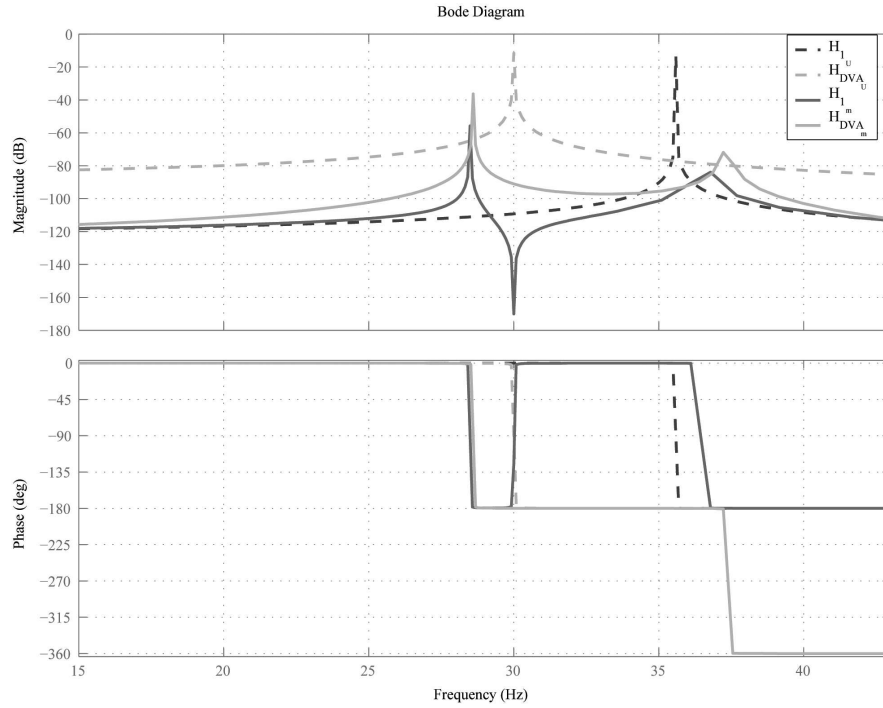


Figure 5.4:  $f_{ext} = 20 \text{ Hz}$ , so  $l_{21} = l_{22} \approx 74 \text{ mm}$

From the maximal acceleration the maximal acceleration force acting on the center of the housing can be derived.

$$\hat{F}_a = m \cdot \hat{a} = 0,5 \text{ kg} \cdot 142 \text{ m/s}^2 = 71 \text{ N} \quad (5.4)$$

To avoid the leaf spring losing contact with the guiding rolls during operation, the four pairs of rolls have to be pre-loaded with about  $18 \text{ N}$  per pair (see figure 5.3(b)). For safety reasons the pre-stress  $F_v$  is chosen to be  $30 \text{ N}$  per pair. The horizontal force required to overcome the friction between the rolls and the leaf spring to move the housing along the spring is given by

Figure 5.5:  $f_{ext} = 30$  Hz, so  $l_{21} = l_{22} \approx 56$  mm

$$\hat{F}_H = \mu(\hat{F}_a + 4F_v) \quad (5.5)$$

The guiding rolls are simple roller bearings made of steel, so the friction factor  $\mu$  is given by 0, 1 (steel/steel, lubricated). This results in a minimal required horizontal force of 19 N. Positioning of the housing is provided by a pulley and a belt glued on the leaf spring. This belt also provides damping (the amount is not estimated) to the DVA and has a width of 25 mm. The pulley has a radius of 17,6 mm, so the outgoing torque of the drive should be at least 0,34 Nm. Between the motor and the pulley a self-inhibiting worm gear with a reduction of 75:1 is placed. In this way the housing is locked to its current position if the motor is switched off. The efficiency factor  $\eta_g$  of the worm gear is 0,2. The ratio between the diameter of the pulley and the diameter of the worm wheel is 1,47:1, so the total reduction of the drive is 110:1. Taking the efficiency of the worm gear into account, the torque transmission ratio becomes 22:1.

$$i = \frac{n_{in}}{n_{out}} = \frac{z_{out}}{z_{in}} = \frac{T_{out}}{T_{in} \cdot \eta_g} \quad (5.6)$$

Thus the minimal required motor torque becomes 16 mNm. Since the friction of the belt and in the drive is not considered, a standard motor with 27,6 mNm is chosen to have little

safety margin. With a working voltage of 24 V this results in a maximal constant rotational speed of 1500 rpm. Therefore the housing can be positioned with 1,3 cm/s. This is only a theoretical value, since slip between the guiding rolls and the leaf spring is not taken into account. So finally the experiments have to show how fast the effective bending length can be changed.

## Chapter 6

# Controller design

This chapter explains the control strategy used to automatically adjust the eigenfrequency of the DVA to the frequency of the excitation force. On each mass an accelerometer is placed and connected to the input of the sound card (analog input) of a computer. Since there are three masses (one primary mass and two secondary masses) three sensors are needed. But the sound card only has two input channels, so a switch is used to change between the accelerometers of the secondary masses. The two actuators (the motors that move the housings) are connected to the parallel port of the computer as well as the switch. This is a digital port, so each pin can only transmit the value 0 or 1. If the value is 0 then the voltage is between 0 V and 1,5 V (this can be set to 0 V by defining an offset) and if the value is 1 then the voltage is between 3 V and 5 V, depending on the computer. As a result the motor can only be turned on and off with one specific voltage. This means that the rotational speed of the motor cannot be controlled, so the housing will be positioned by calculating the required time the motor has to be turned on. All computational work is done by the Data Acquisition Toolbox of Matlab. The control diagram is given in figure 6.1 and the connection circuit diagram can be found in figure 6.3.

At first the actual eigenfrequency of the housings of the DVA are needed. Therefore the frequency response function (FRF) of the DVA is determined, without having the design mounted on the primary mass. One housing is fixed and the other is pushed down and suddenly released. In this way the housing starts to vibrate and the FRF is measured until the housing stops vibrating. The same is done for the other housing. From the eigenfrequency of each wing of the design the position of the housings can be estimated. This information is required later on to determine how far the housing has to be moved to adjust its eigenfrequency to the excitation frequency.

Having determined the actual position of the housings the analog input is started and the measurement is triggered. The measurement lasts until a predetermined number of samples are acquired. After that the function *detFFTqdata.m* is called. This function extracts the measured data from the memory, imports it to the Matlab workspace and stops the analog input. That avoids measuring while moving the housings. Note that the port is only

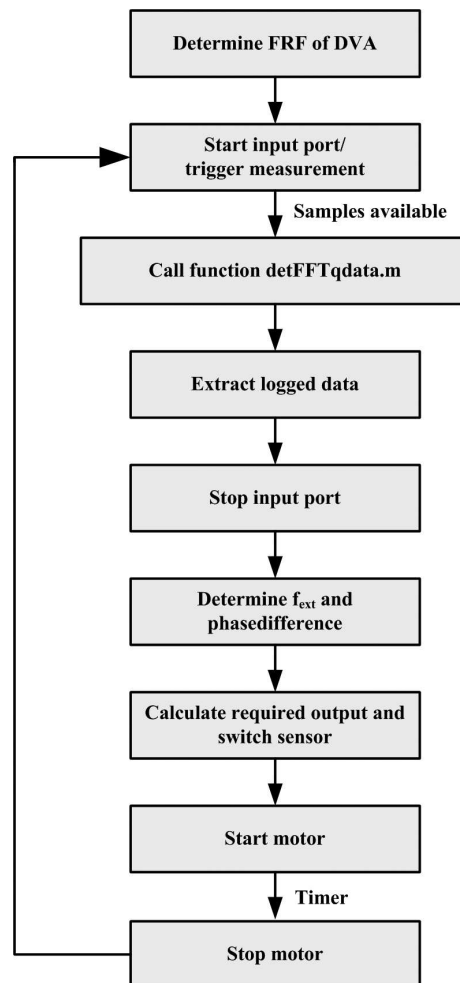


Figure 6.1: Control sequence

stopped but not deleted, since it will be needed again later on. Furthermore the function calculates the power spectrum of the acceleration signal of the secondary mass from which the excitation frequency  $f_{ext}$  is estimated. Beside that the cross spectral density function between the secondary and the primary mass is calculated. Dividing the power spectral density (PSD) of the DVA by the cross spectral density (CSD) of the DVA and the primary mass at the excitation frequency yields the transfer function between the primary and the secondary mass at this frequency. From this transfer function the actual phase difference between the DVA and the primary mass is calculated. Looking for example at figure 5.5 it becomes clear that if this phase difference is zero, the eigenfrequency of the DVA has to be lowered and if the phase difference is  $-180^\circ$  the eigenfrequency of the DVA has to be increased. Only if the phase difference is  $-90^\circ$ , the eigenfrequency of the DVA is equal to the excitation frequency so that the vibrations are suppressed as good as possible. The function *detFFTqdata.m* now calculates the required output to set the eigenfrequency of the DVA or

in other words to position the housing, so that the eigenfrequency of the DVA matches the excitation frequency. The strategy used can be found in figure 6.2.

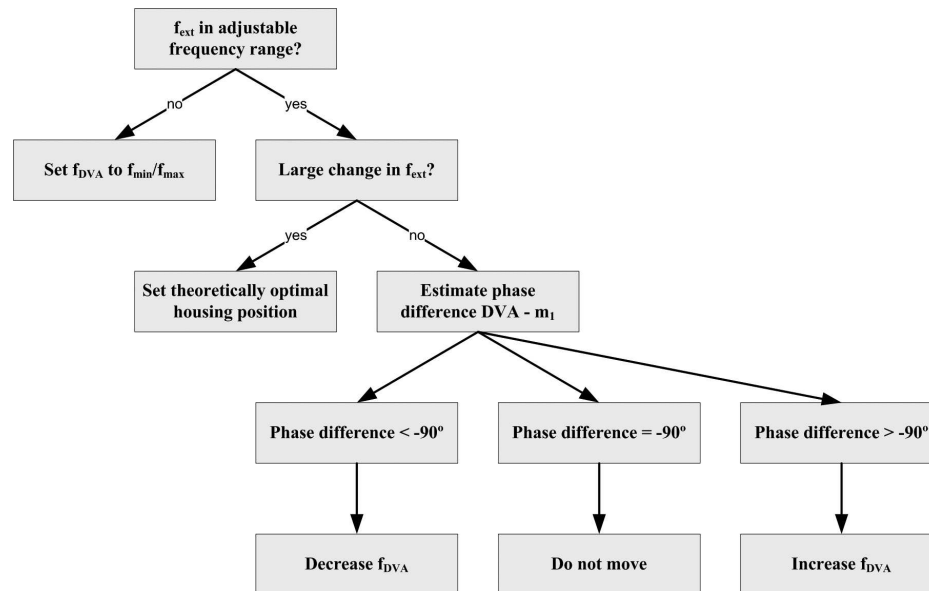


Figure 6.2: Control strategy

At first it is checked whether the excitation frequency is outside the frequency region the eigenfrequency of the DVA can be set in. If the excitation frequency is too low/high, the eigenfrequency of the DVA will be set to the lowest/highest frequency that can be achieved. In this way the housings are prevented from moving into the bearing construction or falling from the leaf spring. If the excitation frequency is inside the adjustable region, the controller checks whether a large change in excitation frequency has occurred. If the excitation frequency compared to the previous measurement changes more than 1 Hz, the theoretically required position of the housing and the time the motor has to be turned on to achieve this position are calculated. In this way the eigenfrequency of the DVA is set near to the excitation frequency. If there is no large change in the excitation frequency and the housing is already set to the theoretically optimal position, the controller uses the information of the phase difference to determine if the actual eigenfrequency of the DVA is equal to the excitation frequency (if the phase difference is  $-90^\circ$  with a certain tolerance). If this is not yet the case, the motor will be turned on in the required direction for a fraction of a second to adjust the position of the housing by a small increment. This has to be done, since the theoretically optimal position is not exact enough in practice. At this moment there is no algorithm available to determine the step size so that the optimal position would be reached faster.

When the function *detFFTqdata.m* has computed the output it switches the actual sensor, so that the acceleration of the other housing of the DVA can be measured next, together with the acceleration of the primary mass. Finally it starts the motor. When the time the

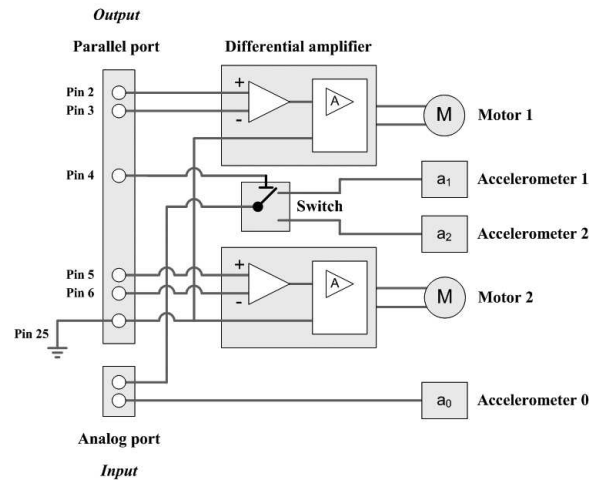


Figure 6.3: Circuit diagram

motor has to be turned on has elapsed, the motor is stopped and a new measurement is started again. The Matlab code for the controller can be found in appendix F.

To be able to estimate the exciting frequency and the phase difference between the DVA and the vibrating machine precisely, the acceleration measurement takes a little time. During the measurement the housings cannot be moved, so the controller is semi-active. Experiments have to show how the controller behaves if the machine vibrates nonlinear. They also have to show which measurement time and which moving speed provides a fast and precise control.

To generate a positive and a negative direction of motor rotation, a differential amplifier is used (see figure 6.3). To control motor 1, pins 2, 3 and 25 are used. If pin 2 and pin 3 have the same value (0 or 1) the difference is 0 V, so the motor will not move. If pin 2 has value 1 and pin 3 is zero, the difference is +3 V (depending on the PC), so the motor will be turned on in the positive rotational direction. If pin 2 is zero and pin 3 is one, the difference is -3 V (depending on the PC), so the motor will rotate in the negative direction. The amplifier is needed to amplify PC's outgoing voltage to the required operational voltage of the motor. The electrical circuit works the same for the second motor. Pin 4 is used to switch between the accelerometers 1 and 2 of the DVA. Accelerometer 0 is placed on the primary mass.

In the next chapter the MMF design and the controller will be tested in practice.

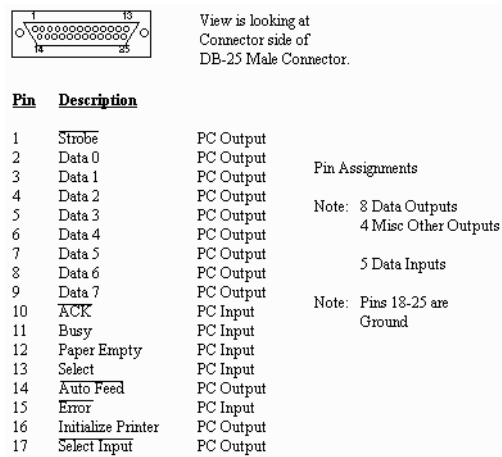


Figure 6.4: Pin assignment of a parallel PC port





## Chapter 7

# Testing the design

After having manufactured the MMF design (see figure 7.2) it is tested in practice. Therefore a primary system representing the vibrating machine is needed. In chapter 5.2 it is already determined that the primary mass should be about 20 kg and the primary spring stiffness should be  $10^6$  N/m.

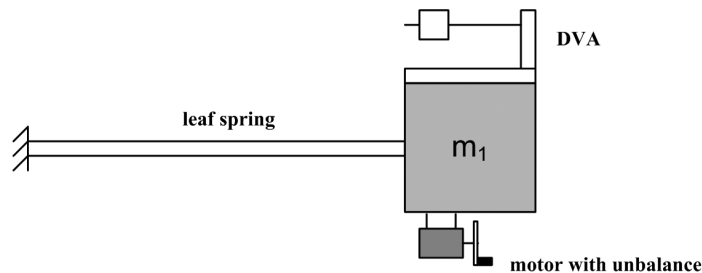


Figure 7.1: Experimental set-up

The primary system consists of a leaf spring clamped at one end. At the other end a mass is located to which the DVA can be mounted (see figure 7.1). The system is excited by a motor with a rotating unbalance. By using (4.12) the geometry of the leaf spring can be determined. The effective length is chosen to be 0,12 m, the width of the spring is 0,18 m and the thickness is 6 mm. This leads to a primary spring stiffness of  $k_1 = 1,18 \cdot 10^6$  N/m. The base area of the primary mass is also  $(20 \times 20)\text{cm}^2$  and a standard steel thickness of 35 mm is chosen. Thus the weight of the primary mass is 22 kg which leads to an eigenfrequency of approximately 37 Hz. This is outside the design region of the DVA. The clamping of the primary leaf spring can be adjusted so the spring stiffness and consequently the eigenfrequency of the primary system can be changed for different experiments if desired.

The excitation force is chosen to be 20 N at 25 Hz. With a rotation radius for the unbalance of 20 mm this leads to a required mass of 40 g, since

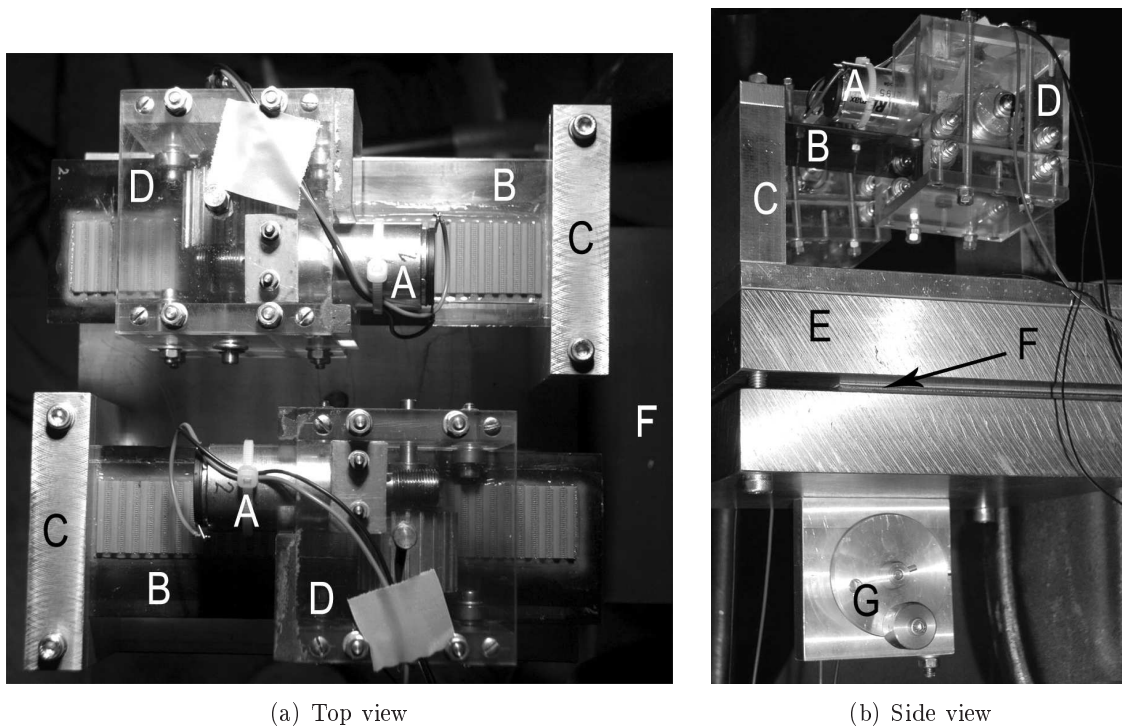


Figure 7.2: Pictures of the manufactured DVA: A = motor, B = secondary leaf spring, C = clamping device, D = housing, E = primary mass, F = primary leaf spring, G = exciting motor

$$F = mr\omega^2 \quad (7.1)$$

Before the DVA is mounted and the controller is tested, some characteristic parameters have to be determined. At first the moving speed of the housings is set to 20 mm/s. Then the eigenfrequency of each housing is measured for certain housing positions. It turns out that the adjustable frequency range of the DVA is about 5 Hz to 11 Hz. This is far less than calculated in chapter 5.2. The reason for the difference is that in theory a point mass acting on the leaf spring is assumed. But in practice the housing is no point mass and the center of the mass is not in the center of the housing. It is near to the motor which results in a moment acting on the spring and introduces inertia. Apart from that the mass of the leaf spring is not taken into account and finally the housings have little play on the belt. But the desired frequency range can be achieved by taking a thicker leaf spring.

Since there is a difference between theory and praxis, the controller cannot determine the required effective length from the measured excitation frequency with (4.14). Thus the measurements for the eigenfrequency of both housings measured for different positions are used to determine a polynomial function to correct the difference between theory and practice to position the housings adequately.

Because of the lower frequency range the DVA is able to be adjusted to, the eigenfrequency of the primary mass is also lowered. It is set to 11,1 Hz so that it can be suppressed by the DVA (the effective leaf spring length is 212 mm). Note that the eigenfrequency of the primary mass will become a little less than 11 Hz if the DVA is mounted, since the weight of the primary mass is 22 kg and the weight of the total DVA with bearing construction is 3,68 kg. The housings have a weight of 0,646 kg and 0,644 kg respectively.

Now the DVA is mounted on the primary mass and the controller is tested. The primary mass is excited with a frequency of 10,7 Hz which is approximately the eigenfrequency for the mounted case. The first thing that becomes clear is that the motor providing the excitation force is mounted in an unsuitable way. By mounting the motor as shown in figure 7.1 the leaf spring is not only bended but also torsion is introduced. As a result the primary mass is not only vibrating up and down but also rotating around the longitudinal axis of the leaf spring. Thus it is decided to change the position of the motor with 90°.

Starting the controller shows that it adjusts the eigenfrequency of both housings to the excitation frequency, although it takes a couple of minutes. The measurement time for determining the excitation frequency and the phase difference between the primary mass and the DVA is set to 20 s. This provides a good measurement. A lower measurement time will cause a worse measurement which will result in a worse controller performance and speed. So this time is the main bottleneck for the controller performance.

Fine tuning with a fixed step size (turning on the motor for 0,02 s coinciding with a displacement of 0,4 mm) results in a long settling time. Therefore a quadratic algorithm is introduced for fine tuning the DVA which returns a large step if the phase difference is far away from  $-90^\circ$  and a small step size if the eigenfrequency of the DVA has almost adapted to the eigenfrequency of the primary system.

The tolerance for controlling the phase difference between the primary mass and the housing is chosen to meet  $10^\circ$ . For the controller it is hard to achieve the desired phase difference, because the system is weakly damped so that the range in which the phase difference changes from  $0^\circ$  to  $-180^\circ$  is very small. Apart from that an interaction between both housings occurs so that the phase of one housing can suddenly change more than  $50^\circ$  if the other housing is moved. To avoid this, a third channel for measuring the acceleration of both housings at the same time is required. In this way the phase difference between the housings can be kept zero. Apart from that the controller will become faster since both housings can be measured at the same time and moved simultaneously. But this is not realized, yet.

The performance of the DVA is shown in figure 7.3. The measurement is done for the eigenfrequency of the primary system in the mounted case (10,7 Hz). Here the DVA reduces the vibration about 65 % (the exact amplitude is unknown since the measurement is not calibrated). Note that the DVA is has not adapted perfectly yet, so there is some capacity left.

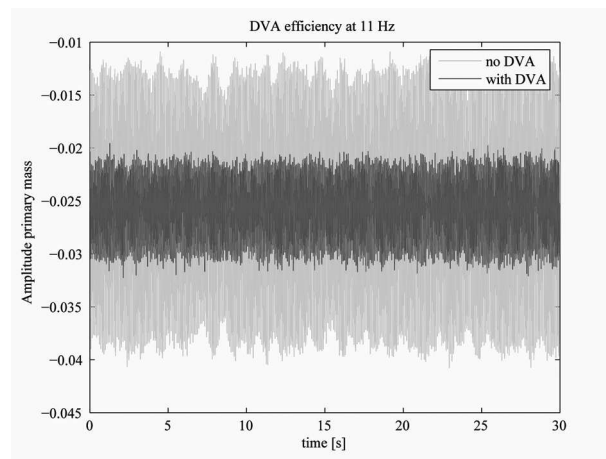


Figure 7.3: Performance of the DVA

## Chapter 8

# Conclusions and recommendations

In this report different types of available DVA's have been studied, but it turns out that none of them meets the stated requirements. Either they are not fail safe or their eigenfrequency cannot be controlled. The eigenfrequency of the standard DVA is not adjustable, the Proof-Mass Actuator can only influence the damping of a system and piezoelectric absorbers and the smart spring design need current to operate. Therefore a new design is developed. Three different possibilities have been presented, namely the cup spring design (combination of cup springs with pre-load adjuster), the satellite design (principle comparable with stretching a guitar string) and the flank design (secondary mass vibrating on a leaf spring with adjustable bending point). The cup spring design is not universal and the satellite design needs a large reduction in the drive and will be heavy because of the high forces required for setting different eigenfrequencies. So finally it is decided to manufacture the flank design. There are two possibilities for designing the flank design: to move the leaf springs or to move the masses. Moving the masses results in a lighter design and the bearing of the leaf springs is easier to realize. This cheap moving mass flank design (MMF design) is modeled and a prototype is made. Furthermore, a controller is designed and a testing construction is built.

Testing the DVA prototype shows that the theoretically estimated adjustable frequency range is not met. This is because in the model inertia of the housing has been neglected although it has a large influence on the eigenfrequency of the DVA. But by taking a thicker leaf spring the adjustable frequency range of the DVA can easily be increased. Although the controller is simple and slow, testing the semi-active DVA shows that a vibration reduction of 65 % is achieved. Unfortunately there was no time to experiment with nonlinearities in the excitation frequency for testing the performance of the DVA.

Finally there are some recommendations. At first a new model for analyzing the MMF design should be made. This model should include the inertia of the housing and the leaf spring mass. In this way the frequency range of the DVA can be estimated more precisely.

The housings of the prototype are made of plexiglass. But since the guiding rolls have to be pre-loaded with 30 N the sides of the housing tend to bend a little under this stress so

that the walls are not perpendicular. Therefore some additional screws have been used to fix the walls. Anyway, the bent walls make positioning the shaft difficult. Thus it is advised to use a stronger kind of plastic or to make the walls thicker. To get rid of play between the housing and the leaf spring one should consider a different drive mechanism. Instead of a pulley and a belt a PU (poly-urethan) drive wheel with high grip on steel could be used.

At the moment only the response to the excitation frequency is measured. The actual position of the housing is estimated by knowing the initial position and updating it every time the housing is moved. This is not very precise and the errors in the position cumulate. With an encoder installed at the motor the actual housing position could be determined constantly. But still the actual corresponding eigenfrequency of the DVA would be unknown. This could be solved by using a proper algorithm for estimating the relation between the housing position and the eigenfrequency of the DVA.

For improving the controller a third input channel should be introduced. Then the acceleration of all masses can be measured at the same time and the housings can be moved simultaneously. This will speed up the controller by a factor two. Apart from that the phase difference between both housings can be controlled, so that the eigenfrequency of the DVA can be set to the exciting frequency more precisely. Finally the algorithms for determining the actual housing position and the appropriate step size for fine tuning the eigenfrequency of the DVA should be improved. In this way a faster controller would be obtained.

# Bibliography

- [BFN04] J. H. Bonsel, R. H. B. Fey, and H. Nijmeijer. Application of a dynamic vibration absorber to a piecewise linear beam system. *Nonlinear Dynamics*, vol. 37, pp. 227-243, 2004.
- [dH56] J.P. den Hartog. *Mechanical Vibrations*. McGraw-Hill, fourth edition, 1956.
- [dKvCo1] Bram de Kraker and Dick H. van Campen. *Mechanical Vibrations*. Shaker Publishing, first edition, 2001.
- [Fla04] Alison B. Flatau, editor. *Smart Systems and Integrated Systems*, volume 5390 of *Smart Structures and Materials*, San Diego, California, USA, 2004. SPIE - The International Society for Optical Engineering.
- [HD79] F. Holzweißig and H. Dresig. *Lehrbuch der Maschinendynamik - Maschinendynamische Probleme und ihre praktischen Lösungen*. Springer Verlag, 1979.
- [Hin90] *Gedämpfte Schwingungen vorgespannter Balken*, volume 142 of *Reihe 11 - Schwingungstechnik*, Düsseldorf, Germany, 1990. VDI Verlag - Verlag des Vereins Deutscher Ingenieure.
- [Mico5] *Micromega Dynamics - Active Damping Devices*. <http://www.micromegadynamics.com>, Aug 16 at 12:31, 2005.
- [NH04] Fred Nietzsche and Tim Harold. Experimental system identification of the smart spring device for semi-active vibration control. *Department of Mechanical and Aerospace Engineering, Carleton University, Ottawa, Ontario K1S 5B6, Canada*, 2004.
- [Pie05] *Piezo Systems Inc*. <http://www.piezo.com>, Aug 18 at 16:12, 2005.
- [Pre02] André Preumont. *Vibration Control of Active Structures - An Introduction*. Kluwer Academic Publishers, second edition, 2002.
- [RM87] Roloff and Matek. *Maschinenelemente - Normung, Berechnung, Gestaltung*. Friedr. Vieweg & Sohn, 1987.





# Appendix A

## List of symbols

Symbol	Description	Unit
$\alpha$	angle	<i>rad</i>
$\eta$	efficiency factor	–
$\mu$	friction factor	–
$\omega_e$	eigenfrequency	<i>rad/s</i>
$\rho$	density	<i>kg/m<sup>3</sup></i>
$\sigma$	stress	<i>Pa</i>
$A$	area	<i>m<sup>2</sup></i>
$a$	length or acceleration	<i>m</i> or <i>m/s<sup>2</sup></i>
$b$	width	<i>m</i>
$c$	stiffness constant	<i>N/m</i>
$d$	damping constant	<i>N/s</i>
$E$	modulus of elasticity	<i>N/m<sup>2</sup></i>
$F$	force	<i>N</i>
$f$	deflection or frequency	<i>m</i> or <i>Hz</i>
$h$	height	<i>m</i>
$I$	momentum of area	<i>m<sup>4</sup></i>
$i$	reduction	–
$k$	spring stiffness constant	<i>N/m</i>
$l$	length	<i>m</i>
$m$	mass	<i>kg</i>
$M$	moment	<i>Nm</i>
$n$	rotational speed	<i>min<sup>-1</sup></i>

Symbol	Description	Unit
$Q$	force	$N$
$r$	radius	$m$
$s$	column compression	$m$
$S$	tensile force	$N$
$t$	time	$s$
$T$	torque	$Nm$
$W$	momentum of bending	$m^3$
$x$	displacement	$m$
$z$	number of teeth	—

## Appendix B

# Eigenfrequency of the satellite design

The derivation of the equation for the eigenfrequency of a pre-stressed beam with an additional mass located at the center is given below. It is based on the linearized vibration equation for a pre-stressed beam without additional mass (see figure B.1). According to Hinrichs [Hing0] this is

$$EI \frac{\partial^4 w}{\partial x^4} - S \frac{\partial^2 w}{\partial x^2} + \rho A \frac{\partial^2 w}{\partial t^2} = 0 \quad (\text{B.1})$$

$$EI w^{IV} - S w'' + \rho A \ddot{w} = 0 \quad (\text{B.2})$$

where  $w(x, t)$  describes the bending line. For the case that an additional mass is added at the center of the beam there are eight boundary conditions. The deflection and the orientation at the beginning and at the end of the beam are zero. At the center the deflection and the orientation has to be the same for either side of the mass. Furthermore the moments acting on the mass have to be in equilibrium, so

$$\begin{aligned} -EI \frac{\partial^2 w_1}{\partial x_1^2} \Big|_{x_1=l} &= -EI \frac{\partial^2 w_2}{\partial x_2^2} \Big|_{x_2=l} \\ \frac{\partial^2 w_1}{\partial x_1^2} \Big|_{x_1=l} &= \frac{\partial^2 w_2}{\partial x_2^2} \Big|_{x_2=l} \\ w_1''(l) &= w_2''(l) \end{aligned} \quad (\text{B.3})$$

In addition the vibration of the mass has to be described by the balance of forces:

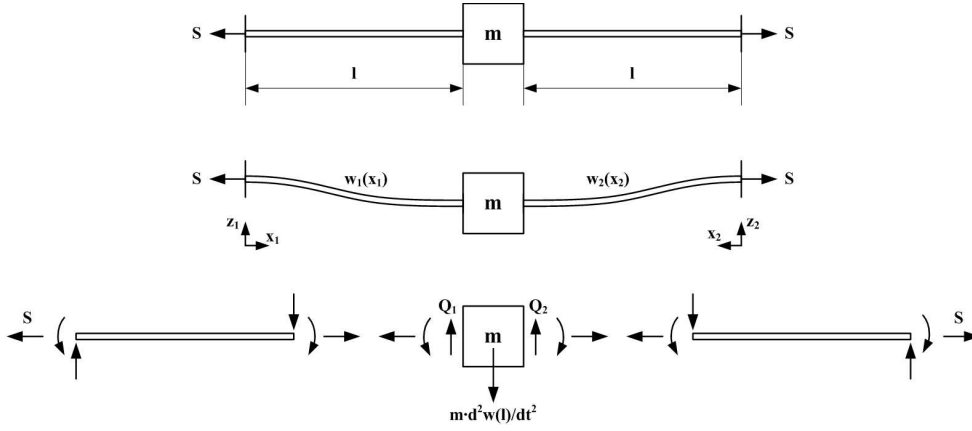


Figure B.1: Load case for a clamped pre-stressed beam with additional mass at the center

$$\begin{aligned}
 m\ddot{w}_1(l) &= m\ddot{w}_2(l) = -Q_1(l) - Q_2(l) \\
 &= -\frac{\partial M_1(l)}{\partial x_1} - \frac{\partial M_2(l)}{\partial x_2} \\
 &= EIw_1'''(l) + EIw_2'''(l) \\
 &= EI [w_1'''(l) + w_2'''(l)]
 \end{aligned} \tag{B.4}$$

This results in the following boundary conditions for all  $t$ :

1.  $w_1(0) = 0$
2.  $w_1'(0) = 0$
3.  $w_2(0) = 0$
4.  $w_2'(0) = 0$
5.  $w_1(l) = w_2(l)$
6.  $w_1'(l) = w_2'(l)$
7.  $w_1''(l) = w_2''(l)$
8.  $m\ddot{w}_1(l) = EI [w_1'''(l) + w_2'''(l)]$

This problem can be simplified by using symmetry. Then the boundary conditions for all  $t$  become:

1.  $w(0) = 0$
2.  $w'(0) = 0$
3.  $w'(l) = 0$
4.  $m\ddot{w}(l) = 2EIw'''(l)$

A solution for the time dependent component of (B.1) is supposed to be given by  $w = W(x)e^{-i\omega t}$ . Substituting this yields

$$EI W^{IV} e^{-i\omega t} - S W'' e^{-i\omega t} + \rho A(-\omega^2)W e^{-i\omega t} = 0 \quad (\text{B.5})$$

$$W^{IV} - \frac{S}{EI} W'' - \omega^2 \frac{\rho A}{EI} W = 0 \quad (\text{B.6})$$

For the x-component a solution is assumed to be given by  $W(x) = \hat{W}e^{i\kappa x}$ , so  $w(x, t) = \hat{W}e^{i(\kappa x - \omega t)}$  is supposed to be a solution to the vibrating beam (B.1). Substituting the solution for the x-component in (B.6) finally yields a characteristic equation for  $\kappa$ .

$$\kappa^4 \hat{W} e^{i\kappa x} + \frac{S}{EI} \kappa^2 \hat{W} e^{i\kappa x} - \omega^2 \frac{\rho A}{EI} \hat{W} e^{i\kappa x} = 0 \quad (\text{B.7})$$

$$\kappa^4 + \frac{S}{EI} \kappa^2 - \omega^2 \frac{\rho A}{EI} = 0 \quad (\text{B.8})$$

This equation has four roots, namely

$$\begin{cases} \kappa_{1,2} = \pm i \sqrt{\frac{S}{2EI} + \sqrt{\left(\frac{S}{2EI}\right)^2 + \omega^2 \frac{\rho A}{EI}}} & := \pm i\kappa_a \\ \kappa_{3,4} = \pm \sqrt{\sqrt{\left(\frac{S}{2EI}\right)^2 + \omega^2 \frac{\rho A}{EI}} - \frac{S}{2EI}} & := \pm \kappa_b \end{cases} \quad (\text{B.9})$$

The final solution to the vibrating beam equation is obtained by superposition of the solutions for the time component and the x-component.

$$w(x, t) = e^{-i\omega t} \left[ \hat{W}_1 e^{i\kappa_1 x} + \hat{W}_2 e^{i\kappa_2 x} + \hat{W}_3 e^{i\kappa_3 x} + \hat{W}_4 e^{i\kappa_4 x} \right] \quad (\text{B.10})$$

$$w(x, t) = e^{-i\omega t} \left[ \hat{W}_1 e^{\kappa_a x} + \hat{W}_2 e^{-\kappa_a x} + \hat{W}_3 e^{i\kappa_b x} + \hat{W}_4 e^{-i\kappa_b x} \right] \quad (\text{B.11})$$

Equation (B.11) can be rearranged by using the relations for trigonometric functions mentioned below.

$$e^{i\alpha} = \cos \alpha + i \sin \alpha \quad (\text{B.12})$$

$$e^{-i\alpha} = \cos \alpha - i \sin \alpha \quad (\text{B.13})$$

$$\sinh \alpha = \frac{1}{2}e^\alpha - \frac{1}{2}e^{-\alpha} \quad (\text{B.14})$$

$$\cosh \alpha = \frac{1}{2}e^\alpha + \frac{1}{2}e^{-\alpha} \quad (\text{B.15})$$

$$\cosh \alpha - \sinh \alpha = e^{-\alpha} \quad (\text{B.16})$$

$$\cosh \alpha + \sinh \alpha = e^\alpha \quad (\text{B.17})$$

Substituting these expressions in (B.11) yields

$$w(x, t) = e^{-i\omega t} [\hat{W}_1(\cosh(\kappa_a x) + \sinh(\kappa_a x)) + \hat{W}_2(\cosh(\kappa_a x) - \sinh(\kappa_a x)) \\ + \hat{W}_3(\cos(\kappa_b x) + i \sin(\kappa_b x)) + \hat{W}_4(\cos(\kappa_b x) - i \sin(\kappa_b x))] \quad (\text{B.18})$$

$$w(x, t) = e^{i\omega t} [a_1 \cos(\kappa_b x) + a_2 \sin(\kappa_b x) + a_3 \cosh(\kappa_a x) + a_4 \sinh(\kappa_a x)] \quad (\text{B.19})$$

Using the four boundary conditions for the symmetric problem gives

1.  $a_1 + a_3 = 0$
2.  $a_2 \kappa_b + a_4 \kappa_a = 0$
3.  $-a_1 \kappa_b \sin(\kappa_b l) + a_2 \kappa_b \cos(\kappa_b l) + a_3 \kappa_a \sinh(\kappa_a l) + a_4 \kappa_a \cosh(\kappa_a l) = 0$
4.  $-m\omega^2 [a_1 \cos(\kappa_b l) + a_2 \sin(\kappa_b l) + a_3 \cosh(\kappa_a l) + a_4 \sinh(\kappa_a l)] \\ = 2EI [a_1 \kappa_b^3 \sin(\kappa_b l) - a_2 \kappa_b^3 \cos(\kappa_b l) + a_3 \kappa_a^3 \sinh(\kappa_a l) + a_4 \kappa_a^3 \cosh(\kappa_a l)]$

These conditions can be described by a linear matrix equation of the form  $K\underline{a} = \underline{0}$ .

$$\begin{bmatrix} 1 & 0 & 1 & 0 \\ 0 & \kappa_b & 0 & \kappa_a \\ -\kappa_b \sin(\kappa_b l) & \kappa_b \cos(\kappa_b l) & \kappa_a \sinh(\kappa_a l) & \kappa_a \cosh(\kappa_a l) \\ \left[ \kappa_b^3 \sin(\kappa_b l) + \frac{m\omega^2}{2EI} \cos(\kappa_b l) \right] & \left[ -\kappa_b^3 \cos(\kappa_b l) + \frac{m\omega^2}{2EI} \sin(\kappa_b l) \right] & \left[ \kappa_a^3 \sinh(\kappa_a l) + \frac{m\omega^2}{2EI} \cosh(\kappa_a l) \right] & \left[ \kappa_a^3 \cosh(\kappa_a l) + \frac{m\omega^2}{2EI} \sinh(\kappa_a l) \right] \end{bmatrix} \begin{bmatrix} a_1 \\ a_2 \\ a_3 \\ a_4 \end{bmatrix} = \begin{bmatrix} 0 \\ 0 \\ 0 \\ 0 \end{bmatrix}$$

Since vector  $\underline{a}$  is non-zero, this equation is satisfied only if  $\det(K) = 0$ . Unfortunately solving this equation symbolically requires too much computational effort. Therefore it can only be solved numerically by using Newtons method, so the values for the variables have to be estimated first.





## Appendix C

# Transfer functions

A transfer function is defined as  $H = \text{output}/\text{input}$ . Here the output is defined to be the displacement of a mass and the input is the exciting force. There are three masses so there are six transfer functions between the displacements and the excitation force, three for the unmounted case and three for the combined systems. At first the transfer functions for the case that the DVA is not mounted will be derived. In this case all systems can be modeled by a single mass-spring-damper system as drawn in figure C.1(a). The equation of motion for the primary mass-damper-spring system is

$$m_1 \ddot{x}_1 + d_1 \dot{x}_1 + k_1 x_1 = F_{ext} \quad (\text{C.1})$$

Applying Laplace transformation yields

$$m_1 s^2 x_1 + d_1 s x_1 + k_1 x_1 = F_{ext} \quad (\text{C.2})$$

Rearranging finally gives the transfer function  $H_{1_u}(s)$  for the primary mass in the unmounted case.

$$H_{1_u}(s) = \frac{x_1}{F_{ext}} = \frac{1}{m_1 s^2 + d_1 s + k_1} \quad (\text{C.3})$$

The same approach is followed to derive the other transfer functions.

$$m_{21} \ddot{x}_{21} + d_{21} \dot{x}_{21} + k_{21} x_{21} = F_{ext} \quad (\text{C.4})$$

$$m_{21} s^2 x_{21} + d_{21} s x_{21} + k_{21} x_{21} = F_{ext} \quad (\text{C.5})$$

$$H_{21_u}(s) = \frac{x_{21}}{F_{ext}} = \frac{1}{m_{21} s^2 + d_{21} s + k_{21}} \quad (\text{C.6})$$

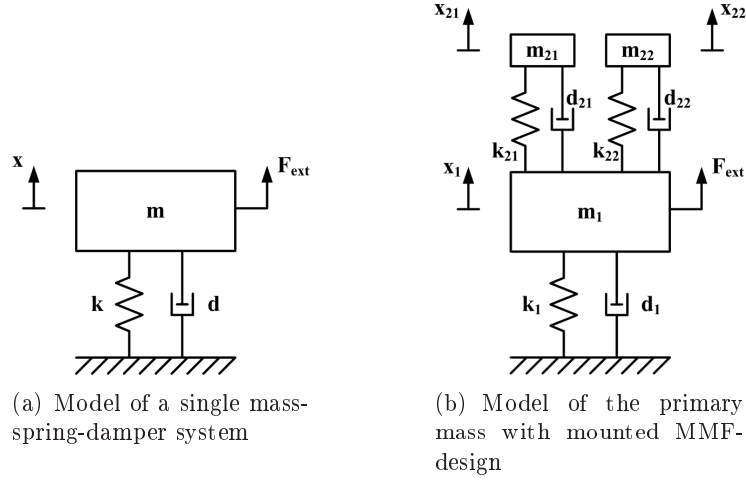


Figure C.1: Models for the unmounted and mounted case

$$m_{22}\ddot{x}_{22} + d_{22}\dot{x}_{22} + k_{22}x_{22} = F_{ext} \quad (\text{C.7})$$

$$m_{22}s^2x_{22} + d_{22}sx_{22} + k_{22}x_{22} = F_{ext} \quad (\text{C.8})$$

$$H_{22_u}(s) = \frac{x_{22}}{F_{ext}} = \frac{1}{m_{22}s^2 + d_{22}s + k_{22}} \quad (\text{C.9})$$

The transfer functions for the mounted case follow from the equations of motion for the coupled systems as described in chapter 4.3.2. The only difference to (4.11) is that damping is also considered now. A model can be found in figure C.1(b).

$$\begin{aligned} m_1\ddot{x}_1 + (d_1 + d_{21} + d_{22})\dot{x}_1 + (k_1 + k_{21} + k_{22})x_1 - d_{21}\dot{x}_{21} - k_{21}x_{21} - d_{22}\dot{x}_{22} - k_{22}x_{22} &= F_{ext} \\ m_{21}\ddot{x}_{21} + d_{21}(\dot{x}_{21} - \dot{x}_1) + k_{21}(x_{21} - x_1) &= 0 \\ m_{22}\ddot{x}_{22} + d_{22}(\dot{x}_{22} - \dot{x}_1) + k_{22}(x_{22} - x_1) &= 0 \end{aligned} \quad (\text{C.10})$$

Applying Laplace transformation yields

$$\begin{aligned} [m_1s^2 + (d_1 + d_{21} + d_{22})s + k_1 + k_{21} + k_{22}]x_1 - d_{21}sx_{21} - k_{21}x_{21} - d_{22}sx_{22} - k_{22}x_{22} &= F_{ext} \\ m_{21}s^2x_{21} + d_{21}s(x_{21} - x_1) + k_{21}(x_{21} - x_1) &= 0 \\ m_{22}s^2x_{22} + d_{22}s(x_{22} - x_1) + k_{22}(x_{22} - x_1) &= 0 \end{aligned} \quad (\text{C.11})$$

For simplicity define

$$[m_1 s^2 + (d_1 + d_{21} + d_{22})s + k_1 + k_{21} + k_{22}]x_1 := A_1(s)x_1 \quad (\text{C.12})$$

Rearranging the equations of motion of the secondary masses and isolating their displacements on one side yields

$$x_{21} = \frac{d_{21}s + k_{21}}{m_{21}s^2 + d_{21}s + k_{21}}x_1 := A_{21}(s)x_1 \quad (\text{C.13})$$

$$x_{22} = \frac{d_{22}s + k_{22}}{m_{22}s^2 + d_{22}s + k_{22}}x_1 := A_{22}(s)x_1 \quad (\text{C.14})$$

Substituting these expressions in the Laplace transformed equation of motion for the primary mass gives an expression for the external force  $F_{ext}$  only depending on  $x_1$ .

$$A_1(s)x_1 - [d_{21}s + k_{21}]x_{21} - [d_{22}s + k_{22}]x_{22} = F_{ext} \quad (\text{C.15})$$

$$[A_1(s) - (d_{21}s + k_{21})A_{21}(s) - (d_{22}s + k_{22})A_{22}(s)]x_1 = F_{ext} \quad (\text{C.16})$$

$$H_{1_m}(s) = \frac{x_1}{F_{ext}} = \frac{1}{A_1(s) - (d_{21}s + k_{21})A_{21}(s) - (d_{22}s + k_{22})A_{22}(s)} \quad (\text{C.17})$$

To derive the transfer function  $H_{21_m}(s)$  for the first secondary mass in the mounted case (C.13) is rearranged and substituted in (C.14).

$$x_1 = \frac{m_{21}s^2 + d_{21}s + k_{21}}{d_{21}s + k_{21}}x_{21} = \frac{1}{A_{21}(s)}x_{21} \quad (\text{C.18})$$

$$x_{22} = A_{22}(s)x_1 = \frac{A_{22}(s)}{A_{21}(s)}x_{21} \quad (\text{C.19})$$

Substituting this in the Laplace transformed equation of motion for the primary mass gives

$$H_{21_m}(s) = \frac{x_{21}}{F_{ext}} = \frac{1}{\frac{A_1(s)}{A_{21}(s)} - (d_{22}s + k_{22})\frac{A_{22}(s)}{A_{21}(s)} - (d_{21}s - k_{21})} \quad (\text{C.20})$$

Analogously the transfer function  $H_{22_m}$  can be derived.

$$x_1 = \frac{m_{22}s^2 + d_{22}s + k_{22}}{d_{22}s + k_{22}}x_{22} = \frac{1}{A_{22}(s)}x_{22} \quad (\text{C.21})$$

$$x_{21} = A_{21}(s)x_1 = \frac{A_{21}(s)}{A_{22}(s)}x_{22} \quad (\text{C.22})$$

$$H_{22_m}(s) = \frac{x_{22}}{F_{ext}} = \frac{1}{\frac{A_1(s)}{A_{22}(s)} - (d_{21}s + k_{21})\frac{A_{21}(s)}{A_{22}(s)} - (d_{22}s - k_{22})} \quad (\text{C.23})$$

Note that if the effective lengths of both leaf springs are the same, the  $H_{21_u} = H_{22_u}$  and  $H_{21_m} = H_{22_m}$ . As an example the transfer functions for one secondary mass adjusted to 30 Hz and the other adjusted to 25 Hz (the effective lengths of the springs differ) are drawn below.

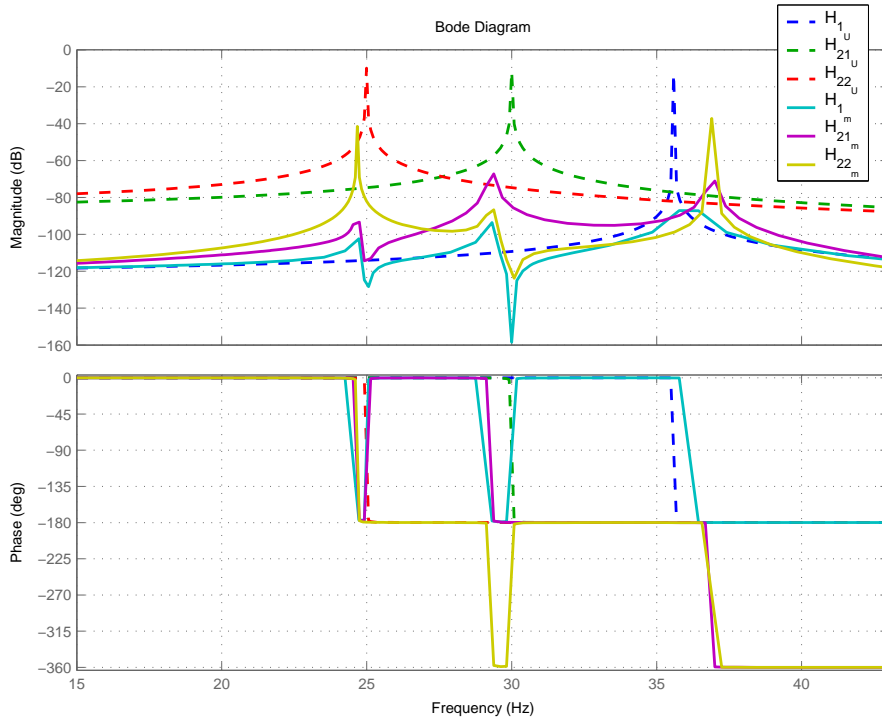
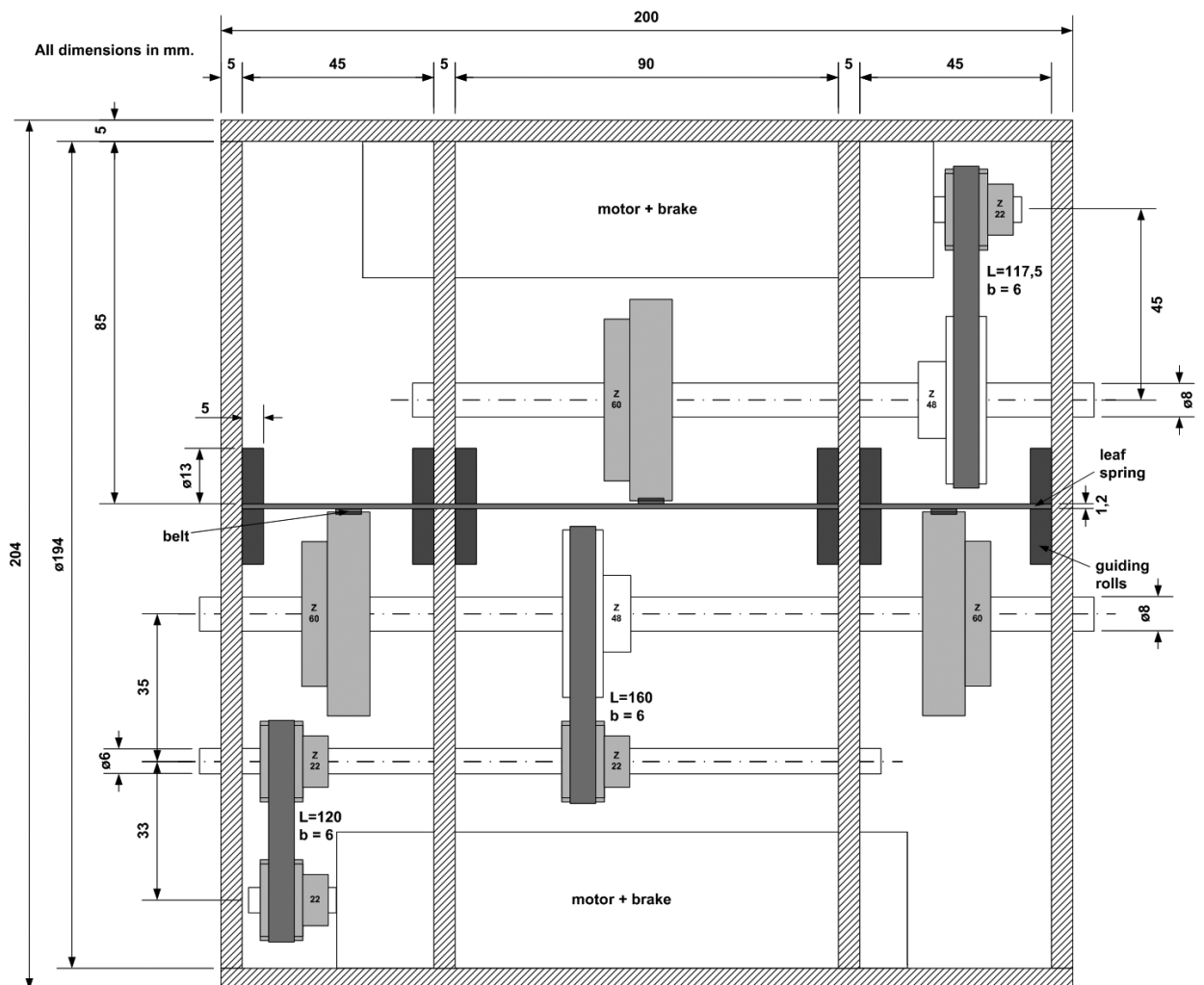


Figure C.2: Example of the transfer functions when the effective lengths of the springs differ.

# Appendix D

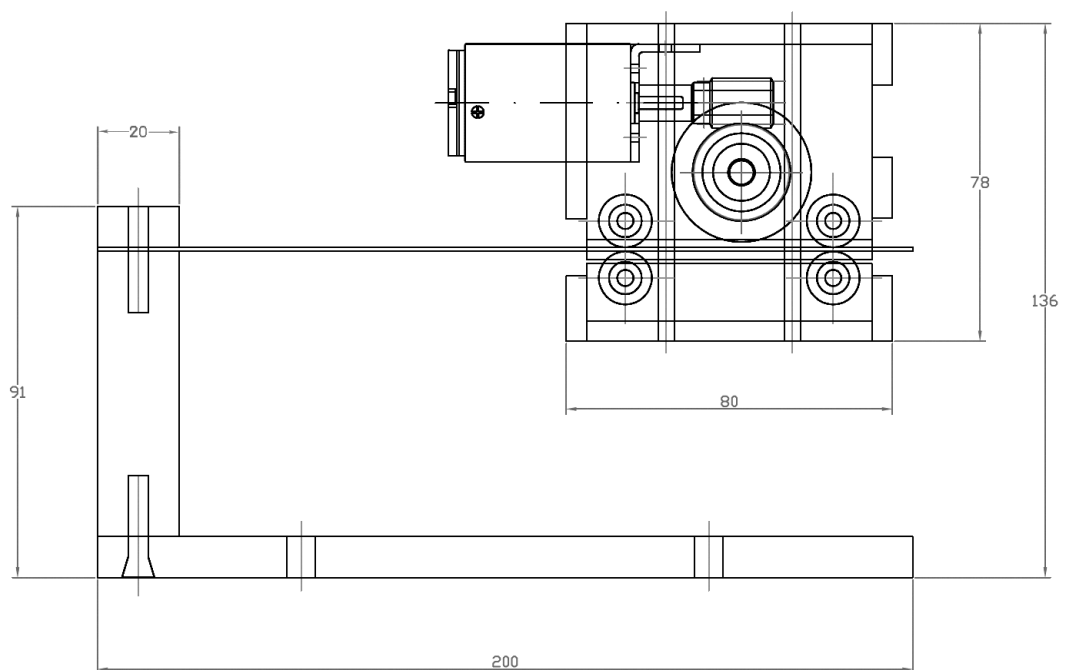
## Construction drawing flank design



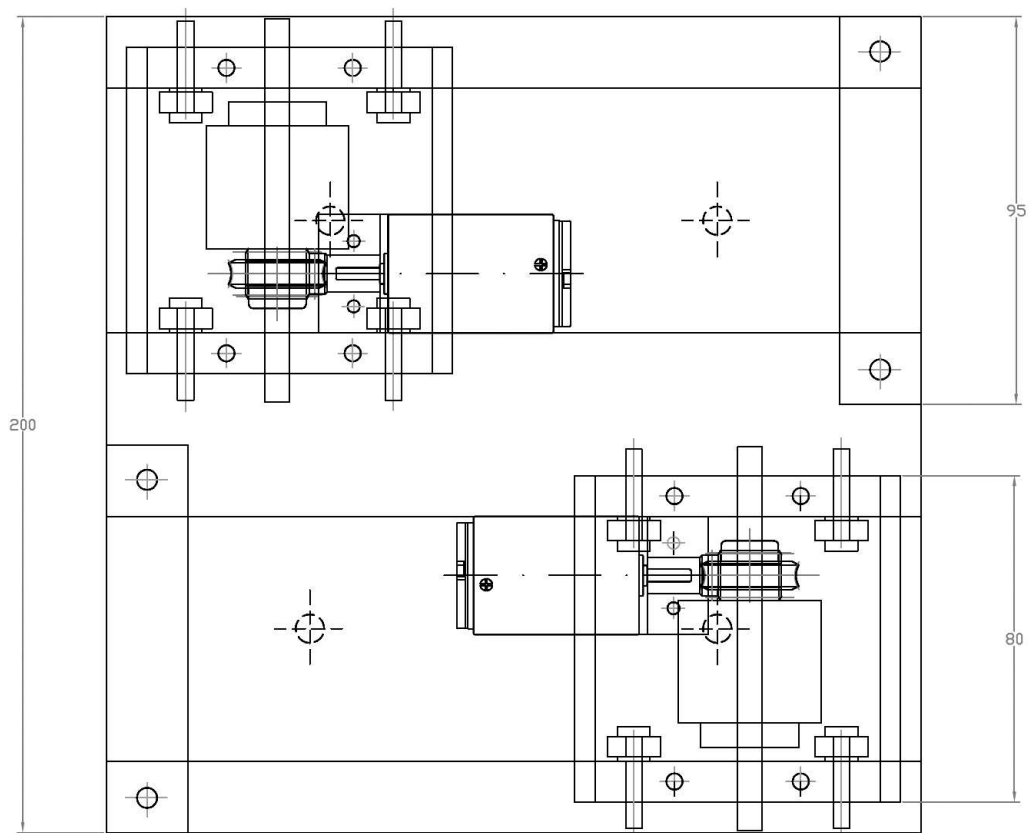


## Appendix E

# Construction drawing mass moving flank design







# Appendix F

## Matlab code for the controller

### F.1 Main program: *controller.m*

```
% This program can be used to control the semi-active MMF design DVA with
% having both wings damping the same frequency (l21 = l22)
%
% To stop running this controller write in the command line
5 %     stop(AI)
%     putvalue(ParPort,[0 0 0 0 0])
%     stop(ParPort)

% Clean workspace:
10 clear all
close all
clc

global E b h m_21 m_22 Fs Fs_fact mtime v0 fmin fmax fext_prev_1 fext_prev_2
15 global fchange l21 l22 S tol

% Declaring constants:
h = 0.001;      % [m]   thickness of the leaf spring
b = 0.06;      % [m]   width of the leaf spring
20 E = 2.1e11;  % [Pa]  E-modulus
m_21 = 0.646;  % [kg]  weight of the housing DVA 1
m_22 = 0.644;  % [kg]  weight of the housing DVA 2
Fs = 8000;     % [Hz]  sample frequency
Fs_fact = 32;  % [-]   samples reduction factor
25 v0 = 20e-3;  % [m/s] housing speed (at 11 V)
fmin = 4.47;  % [Hz]  minimal frequency that can be damped
fmax = 11;     % [Hz]  maximal frequency that can be damped
fchange = 1;   % [Hz]  if change in fext > fchange, housing is moved fast
mtime = 20;    % [s]   measurement time
30 tol = 10;    %f []   tolerance for phase difference precision

% Insert data from determineFRF.m here:
f1 = 6.12;     % [Hz]  eigenfrequency of m21
f2 = 6.12;     % [Hz]  eigenfrequency of m22
35

% Initialization:
S = 0;         % [-]   ID of actual DVA accelerometer
l21 = 92e-3;   % [m]   Initial position DVA 1
```

```

122 = 92e-3; % [m] Initial position DVA 1
40 fext_prev_1 = f1; % [Hz] set previous value for excitation frequency fext of ←
    m21
fext_prev_2 = f2; % [Hz] set previous value for excitation frequency fext of ←
    m22

% omega21 = 2*pi*f1;
45 % omega22 = 2*pi*f2;
%
% % Estimate actual position/effective length of m21
% l21 = (E*b*h^3/(4*m_21*omega21^2))^(1/3);
% l_pract1 = 1E-05*l21^3 - 0,0066*l21^2 + 2,2134*l21 - 130,27;
50 % l21 = l_pract1;
% % Estimate actual position/effective length of m22
% l22 = (E*b*h^3/(4*m_22*omega22^2))^(1/3);
% l_pract2 = 3E-06*l22^3 - 0,0034*l22^2 + 1,8388*l22 - 115,78;
% l22 = l_pract2;
55

% % Get general information about the sound card
% out = daqhwinfo('winsound')
60 % out.ObjectConstructorName(:) % AI supported?

% Find any open DAQ objects and stop them.
65 openDAQ = daqfind;
for i = 1:length(openDAQ),
    stop(openDAQ(i));
end
clear openDAQ % clear from MATLAB Workspace
70

%%%%%%%%%%%%%%
% MAIN PROGRAM %
%%%%%%%%%%%%%%

75 AI = analoginput('winsound'); % declare input
chan_acc_M1 = addchannel(AI,1); % accelerometer primary mass
chan_acc_M2 = addchannel(AI,2); % accelerometer secondary mass
ParPort = digitalio('parallel','LPT1'); % declare output
80 addline(ParPort,0:4,'out');

% The output vector is defined as
% [motor_1_pos, motor_1_neg, switch, motor_2_pos, motor_2_neg]
% The values for the channels can be set to 0 or 1.
85 %
% motor_1_pos = 1 => motor turned on in positive direction (higher feig_DVA)
% motor_1_neg = 1 => motor turned on in negative direction (lower feig_DVA)
% switch S = 0 => DVA accelerometer on housing 1 active
% switch S = 1 => DVA accelerometer on housing 2 active
90 % motor_2_pos = 1 => motor turned on in positive direction (higher feig_DVA)
% motor_2_neg = 1 => motor turned on in negative direction (lower feig_DVA)
%
%
%
% L=0 L=1
95 %
% xI <- pos. I I
% xI=====I DVA I=====
% xI I-----I -> neg.

```

```

100 % <- pos. motor direction, feig_DVA becomes higher, delta_L is negative
    % -> neg. motor direction, feig_DVA becomes lower, delta_L is positive
    %
    % delta_L = l_req - l (required effective length - actual effective length)
105
    % Use manual triggers when starting multiple device objects because this
    % trigger type executes faster than other trigger types with the exception
    % of hardware triggers. Additionally, to synchronize the input and output
110 % of data, the ManualTriggerHwOn property to Trigger for AI is configured.
    set(AI,'TriggerType','Manual')
    set(AI,'ManualTriggerHwOn','Trigger')
    set(AI,'SampleRate',Fs)
    set(AI,'SamplesPerTrigger',mtime*Fs)
115
    % Define the callback function detFRFqdata when the samples are acquired,
    % and call daqcallback when AI stops running. Call qoutput to turn of the
    % motor after a specific time t which is defined in detFRFqdata.
    set(AI,'SamplesAcquiredFcn',{@detFFTqdata, ParPort})
120 set(AI,'SamplesAcquiredFcnCount',Fs*mtime)
    set(AI,'StopFcn',@daqcallback)
    % set(ParPort,'TimerFcn',{@qoutput, AI})

125
    %%%%%%%%%%%%%%%%%%%%%%%%%%%%%%%%%%%%%%%%%
    % START CONTROLLER %
    %%%%%%%%%%%%%%%%%%%%%%%%%%%%%%%%%%%%%%%%%
130 % softscope(AI)

    start(ParPort)

    start(AI)
135 trigger(AI)
    display('Controller started')
    display('Acquisition started')

```

## F.2 Processing data: function `detFFTqdata.m`

```

% This function gets the sampled data and stops the acquisition. It
% determines the excitation frequency and the phase difference between
% primary mass and DVA and calculates the required output. Finally it
% switches the accelerometer and truns on the motor.
5
function detFFTqdata(obj,event,ParPort)

global E b h m_21 m_22 Fs Fs_fact mtime v0 fmin fmax fext_prev_1 fext_prev_2
global fchange l21 l22 S tol
10
display(S)

%%%%%%%%%%%%%%%%%%%%%%%%%%%%%%%%%%%%%%%%
% INPUT DATA %
15 %%%%%%%%%%%%%%%%%%%%%%%%%%%%%%%%%%%%%%%%%

% Acquire data: column 1 = acc_m1, column 2 = acc_DVA
[data, time] = getdata(obj,Fs*mtime);

```

```

display('Data acquired')
20
% decimate data
d = data;
data = [];
data = decimate(d(:,1),Fs_fact);
25 data = [data, decimate(d(:,2),Fs_fact)];
time = decimate(time,Fs_fact);

% RMS_acc1 = norm(data(:,1))/sqrt(length(data))
% RMS_acc2 = norm(data(:,2))/sqrt(length(data))
30 %
% figure(1)
% plot(time,data)

35 %%%%%%%%%%%
% Determine FFT and FRF %
%%%%%%%%%%

% [Pm1, fml] = psd(data(:,1), [], Fs/Fs_fact);
40 % [maxPm1, i1] = max(Pm1(3:length(Pm1)));

[PDVA, fDVA] = psd(data(:,2), [], Fs/Fs_fact);
[maxPDVA, i2] = max(PDVA(3:length(PDVA)));

45 % figure(2)
% plot(fDVA, PDVA)

C = csd(data(:,1), data(:,2), [], Fs/Fs_fact);
% H1 = Pm1./C;
50 H2 = PDVA./C;

% mag1 = 20*log(abs(H1));
% ang1 = 180/pi*angle(H1);
mag2 = 20*log(abs(H2));
55 ang2 = -180/pi*angle(H2);

% Determine phase differnece between m1 and DVA at excitation frequency
% phase = ang1(i1);
phase = ang2(i2+2)

60 fext = fDVA(i2+2) % excitaition frequency

65 %%%%%%%%%%%
% OUTPUT DATA %
%%%%%%%%%%

if S == 0
70   if or(fext <= fmin, fext >= fmax)
       % fext outside adjustable frequency range
       display('fext outside adjustable frequency range')
       if fext <= fmin
           l_req = (E*b*h^3/(4*m_21*(2*pi*fmin)^2))^(1/3);
75       l_pract1 = (1E-05*(l_req*10^3)^3 - 0.0066*(l_req*10^3) ←
                   ^2 + 2.2134*(l_req*10^3) - 130.27)*1.1;
           l_req = l_pract1*10^-3;
       elseif fext >= fmax
           l_req = (E*b*h^3/(4*m_21*(2*pi*fmax)^2))^(1/3);
           l_pract1 = (1E-05*(l_req*10^3)^3 - 0.0066*(l_req*10^3) ←

```

```

      ^2 + 2.2134*(l_req*10^3) - 130.27)*1.1;
80     l_req = l_pract1*10^-3;
     end

     if abs(l_req-121) > 0.1e-3
       delta_l = l_req - 121;
85       t = abs(delta_l/v0);
       if delta_l < 0
         motor = [1 0];
       elseif delta_l > 0
90         motor = [0 1];
       end
     else motor = [0 0];      % feig_DVA already set to limit value,
       delta_l = 0;          % so do not turn on motor.
       t = 0.1;             % Wait t sec. before starting measurement ←
       again
       display('Limit frequency already set')
95     end

     elseif and(abs(fext_prev_1 - fext) > fchange, and(fext > fmin, fext < fmax ←
    ))
       % large change in fext
       display(fext_prev_1)
100      display('large change in fext')
       l_req = (E*b*h^3/(4*m_21*(2*pi*fext)^2))^(1/3);
       l_pract1 = (1E-05*(l_req*10^3)^3 - 0.0066*(l_req*10^3)^2 + 2.2134*( ←
         l_req*10^3) - 130.27)*1.1;
       l_req = l_pract1*10^-3;
       delta_l = l_req - 121
105       t = abs(delta_l/v0);
       if delta_l < 0
         motor = [1 0];
       elseif delta_l > 0
         motor = [0 1];
110       else display('No WAY')
       end

     else display('Fine tuning')
       if phase > -90+tol      % feig_DVA > fext
115         motor = [0 1];      % Turn on motor in negative direction
         t = (3*10^-5*abs(phase+90)^2 + 0.0027*abs(phase+90) + 4*10^-15)*.9
         delta_l = t*v0;
       elseif phase < -90-tol % feig_DVA < fext
         motor = [1 0];      % Turn on motor in positive direction
120         t = (3*10^-5*abs(phase+90)^2 + 0.0027*abs(phase+90) + 4*10^-15)*.9
         delta_l = -t*v0;
       else motor = [0 0];    % Do not turn on motor.
         delta_l = 0;
         t = 0.1;           % Wait t sec. before starting measurement ←
         again
125       end
     end

     S = 1;                  % Switch actual sensor
     % Update actual position/effective length of m21 and f_ext_prev_1
130     l21 = l21 + delta_l;
     fext_prev_1 = fext;
     output = [motor S 0 0];

     elseif S == 1
135       if or(fext <= fmin, fext >= fmax)
         % fext outside adjustable frequency range

```

```

display('fext outside adjustable frequency range')
if fext <= fmin
    l_req = (E*b*h^3/(4*m_22*(2*pi*fmin)^2))^(1/3);
    l_pract2 = (3E-06*(l_req*10^3)^3 - 0.0034*(l_req*10^3) ←
        ^2 + 1.8388*(l_req*10^3) - 115.78)*1.1;
    l_req = l_pract2*10^-3;
elseif fext >= fmax
    l_req = (E*b*h^3/(4*m_22*(2*pi*fmax)^2))^(1/3);
    l_pract2 = (3E-06*(l_req*10^3)^3 - 0.0034*(l_req*10^3) ←
        ^2 + 1.8388*(l_req*10^3) - 115.78)*1.1;
    l_req = l_pract2*10^-3;
end

if abs(l_req-122) > 0.1e-3
    delta_l = l_req - 122;
    t = abs(delta_l/v0);
    if delta_l < 0
        motor = [1 0];
    elseif delta_l > 0
        motor = [0 1];
    else display('delta_l == 0')
    end
else motor = [0 0];      % feig_DVA already set to limit value,
    delta_l = 0;        % so do not turn on motor.
    t = 0.1;           % Wait t sec. before starting measurement ←
    again
    display('Limit frequency already set')
end

elseif and(abs(fext_prev_2 - fext) > fchange, and(fext > fmin, fext < fmax ←
))
    % large change in fext
    display(fext_prev_1)
    display('large change in fext')
    l_req = (E*b*h^3/(4*m_22*(2*pi*fext)^2))^(1/3);
    l_pract2 = (3E-06*(l_req*10^3)^3 - 0.0034*(l_req*10^3)^2 + 1.8388*( ←
        l_req*10^3) - 115.78)*1.1;
    l_req = l_pract2*10^-3;
    delta_l = l_req - 122;
    t = abs(delta_l/v0);
    if delta_l < 0
        motor = [1 0];
    elseif delta_l > 0
        motor = [0 1];
    end

else display('Fine tuning')
    if phase > -90+tol      % feig_DVA > fext
        motor = [0 1];    % Turn on motor in negative direction
        t = (3*10^-5*abs(phase+90)^2 + 0.0027*abs(phase+90) + 4*10^-15)*.9
        delta_l = t*v0;
    elseif phase < -90-tol % feig_DVA < fext
        motor = [1 0];    % Turn on motor in positive direction
        t = (3*10^-5*abs(phase+90)^2 + 0.0027*abs(phase+90) + 4*10^-15)*.9
        delta_l = -t*v0;
    else motor = [0 0];    % Do not turn on motor.
        delta_l = 0;
        t = 0.1;         % Wait t sec. before starting measurement ←
        again
end
end
end

```

```

195     S = 0;                                % Switch actual sensor
        % Update actual position/effective length of m22 and f_ext_prev_2
        l22 = l22 + delta_1;
        fext_prev_2 = fext;
        output = [0 0 S motor];

200     end

        display(output)

        % set(ParPort,'TimerPeriod',t)
        %
205     % putvalue(ParPort,output);
        % display('Output sent')

        time = cputime;
        while cputime-time < t
210             putvalue(ParPort,output);
        end
        putvalue(ParPort,[0 0 S 0 0]);          % Trun off motor
        display('Output finished')
        display('=====')

215     start(obj)
        trigger(obj)
        display('Acquiring data')

220     % The output vector is defined as
        % [motor_1_pos, motor_1_neg, switch, motor_2_pos, motor_2_neg]
        % The values for the channels can be set to 0 or 1.
        %
225     % motor_1_pos = 1 => motor turned on in positive direction (higher feig_DVA)
        % motor_1_neg = 1 => motor turned on in negative direction (lower feig_DVA)
        % switch      = 0 => DVA accelerometer on housing 1 active
        % switch      = 1 => DVA accelerometer on housing 2 active
        % motor_2_pos = 1 => motor turned on in positive direction (higher feig_DVA)
230     % motor_2_neg = 1 => motor turned on in negative direction (lower feig_DVA)

```